Optimizing Unitary Coupled Cluster Wave Functions on Quantum Hardware: Error Bound and Resource-Efficient Optimizer

Martin Plazanet^{1,2,3,4} and Thomas Ayral¹

In this work, we study the projective quantum eigensolver (PQE) approach to optimizing unitary coupled cluster wave functions on quantum hardware, as introduced in [36]. The projective quantum eigensolver is a hybrid quantum-classical algorithm which, by optimizing a unitary coupled cluster wave function, aims at computing the ground state of many-body systems. Instead of trying to minimize the energy of the system like in the variational quantum eigensolver, PQE uses projections of the Schrödinger equation to efficiently bring the trial state closer to an eigenstate of the Hamiltonian. In this work, we provide a mathematical study of the algorithm, which allows us to obtain a number of interesting results. We first show that one can derive a bound relating off-diagonal coefficients (residues) of the Hamiltonian to the error of the algorithm. This bound not only gives a formal motivation to the projective approach to optimizing unitary coupled cluster wavefunctions, but it also allows us to formulate a well-informed convergence criterion for residue-based optimizers. We then introduce a mathematical study of the classical optimization itself, and show that, using our results, one can derive a residue-based optimizer for which we present numerical evidence of superiority over both the optimization introduced in [36] and VQE optimized using the Broyden-Fletcher-Goldfarb-Shanno (BFGS) method.

Simulating quantum many-body physics is the prime motivation behind the inception of quantum computing [11]. The main premise of quantum computers is that a time evolution of these artificial quantum systems [23]—with the laws of quantum mechanics built-in—will not be plagued with the computational bottlenecks attached to mimicking these dynamics with classical computers [3]. Yet, the experimental quantum processors that have appeared in

the recent years must reckon with decoherence, an unavoidable byproduct of the very laws that afford a quantum acceleration. With quantum error correction still a long way ahead despite very promising recent experimental efforts [1, 8, 9, 20], textbook quantum algorithms like quantum phase estimation [18], whose main ingredient is the aforementioned time evolution, are rendered virtually useless by decoherence because of the duration, often measured in terms of the gate count, of the corresponding quantum circuit.

This practical hurdle has prompted the revival of the standard variational method in a quantum context: while the quantum processor is used to prepare a possibly complex parametric quantum state and to measure the corresponding variational energy, the new parameters are determined by a classical optimization algorithm. This hybrid algorithm, called the variational quantum eigensolver (VQE, [31], see [37] for a review), a priori allows one to pick a variational state whose preparation on the quantum processor will be faster than decoherence, while being complex enough that its energy would be hard to measure on a classical processor alone. However, recent research efforts have unveiled a number of issues with VQE. (i) decoherence: it sharply limits the size of circuits that can be run in practice and therefore their expressivity. Beyond compilation efforts to shorten a given state preparation with sophisticated optimizations of the circuit at hand, adaptive ansatz construction methods [12] or orbital optimization methods [5, 6, 28, 29, 33] have been developed to make the most of the available coherence. But even without decoherence, VQE would still suffer from (ii) the measurement problem: measuring the variational energy involves computing the empirical means of quantum measurement outcomes, yielding a central-limit-theorem-induced $1/\epsilon^2$ dependence of the run time on the statistical error ϵ , leading to prohibitively long run time estimates for relevant quantum chemistry problems [39]. Improvements over plain vanilla energy estimation like term grouping [37, Section 5] or classical shadows [15] improve the prefactor but do not alter this $1/\epsilon^2$

¹Eviden Quantum Lab, Les Clayes-sous-Bois, France

²Centre for Quantum Technologies, National University of Singapore, Singapore 117543, Singapore

³École Polytechnique, I.P. Paris, F-91120 Palaiseau, France

⁴MajuLab, CNRS-UCA-SU-NUS-NTU International Joint Research Laboratory

dependence. Lastly, VQE can be plagued with (iii) an optimization problem, namely by the hardness of finding the global minimum of the variational energy. Very long, and thus potentially very expressive, state preparation circuits like so-called hardware-efficient ansätze [17] tend to be close to random, which leads to a cost landscape that is exponentially flat with the number of orbitals (qubits) [21, 32]. This "barren plateau" phenomenon [25] is but an average statement, and could therefore be escaped with carefully initialized, and/or physically motivated variational states. Yet, even in the absence of this problem, the precise behavior of the optimization is a still largely uncharted territory. In particular, the number of steps to convergence and the distance to the true ground state energy are in general unknown.

Facing these issues, two main routes have been taken thus far. A first route consists in turning back to quantum phase estimation algorithms and, waiting for quantum error corrected computers, optimizing the various building blocks of the algorithm to reduce the requisite resources. This is arguably a very long term strategy given the chasm between the number of physical qubits required for such a quantum error corrected approach [7, 38], and the number of physical qubits achieved in recent experiments [1]. Also, a prerequisite for an efficient quantum phase estimation is an input state with a large enough overlap with the sought-after ground state. Finding such an input state is probably difficult for very correlated systems [22, 24]. This underlines the importance of the second route, which consists in devising ground state preparation strategies suited for current or nearterm processors. This route relies on the hope either that quantum advantage can be squeezed out of these processors in the near term, or that such methods will anyway be needed to produce good enough input states for error-corrected algorithms, implemented on fault-tolerant processors, like phase estimation.

Recent representatives of this second route include recent works like that of [34] that supposedly eschew the optimization and measurement problems by not performing any optimization on the quantum computer (the optimal parameters found by a classical method are fed to a quantum ansatz without reoptimization) and by not attempting the estimation of the energy on the quantum computer, but instead use the quantum processor to select important subspaces, which a classical supercomputer then diagonalizes.

Another method, which will be the focus of this work, turns away from the variational principle and instead, taking direct inspiration from the numerical solution of coupled cluster equations [41] on classical computers, formulates ground state search as a root-finding problem. This method, dubbed the projective quantum eigensolver (PQE), was introduced in [36]. Its superiority in terms of speed compared to VQE was checked on a few example systems using numer-

ical simulations. [36] also mentions the existence of an error bound. The algorithm was also implemented recently [26] on superconducting hardware.

In this paper, we build on the promising properties of PQE, namely the faster convergence observed in the numerical benchmarks, and the purported existence of error bounds, which indicate the algorithm could possibly not suffer from phenomena such as local minima. Here, we provide rigorous and tighter error bounds for PQE. We then introduce a mathematical study of quasi-Newton methods for PQE, ultimately allowing us to introduce a novel optimization method with a faster and more robust convergence. We provide extensive numerical benchmarks showing the superiority in resource cost of this method over both VQE optimized using the Broyden–Fletcher–Goldfarb–Shanno (BFGS) method, and the original optimization for PQE proposed in [36].

The paper is structured as follows: In the first section we summarize the projective quantum eigensolver approach as introduced in [36] as well as our main results. In the second section we introduce an error bound for the algorithm, and discuss its implications and utility. In a third section, we introduce a mathematical study of quasi-Newton algorithms and discuss its implications. In the last part, we introduce our own, more robust and resource-efficient optimization method.

1 Summary of the projective quantum eigensolver method and of our results

1.1 The Algorithm

In this section we briefly summarize the projective quantum eigensolver method introduced by [36].

We are considering an interacting system with m fermionic modes described by the electronic structure Hamiltonian:

$$\hat{H} = \sum_{pq=1}^{m} h_{pq} \hat{a}_{p}^{\dagger} \hat{a}_{q} + \frac{1}{2} \sum_{pqrs=1}^{m} v_{pqrs} \hat{a}_{p}^{\dagger} \hat{a}_{q}^{\dagger} \hat{a}_{s} \hat{a}_{r}, \quad (1)$$

where h_{pq} is a one-body integral, v_{pqrs} a two-body integral, and \hat{a}_p^{\dagger} and \hat{a}_q respectively create and annihilate electrons in the corresponding spin-orbitals. We wish to compute this Hamiltonian's ground state energy E_0 by optimizing a parametric representation $|\Psi(t)\rangle = \hat{U}(t) |\Phi_0\rangle$ of the many-body wavefunction, with $|\Phi_0\rangle$ a reference state (usually taken to be the Hartree-Fock state), and $\hat{U}(t)$ a unitary parameterized by parameters $t \in \mathbb{R}^N$.

The number N of parameters is assumed to be much smaller than the Hilbert space size, $N \ll 2^m$, to benefit from a compressed (not exponentially costly) representation of the wavefunction and to enable (although not guarantee) an efficient optimization process. Here, as in [36] and in many quantum chemical

approaches, we shall use a variant of the unitary coupled cluster ansatz often referred to as 'disentangled' [10]:

$$\hat{U}(t) = \prod_{\mu \in \mathcal{A}} e^{t_{\mu} \hat{\kappa}_{\mu}}, \tag{2}$$

where the generators $\hat{\kappa}_{\mu}$ read $\kappa_{\mu} = \hat{\tau}_{\mu} - \hat{\tau}_{\mu}^{\dagger}$, with excitation operators $\tau_{(i,j,\cdots)(a,b,\cdots)} = \hat{a}_a^{\dagger} \hat{a}_b^{\dagger} \cdots \hat{a}_j \hat{a}_i$, representing an excitation from occupied orbitals i,j,\ldots to unoccupied orbitals a,b,\ldots . The pool \mathcal{A} of excitations we use is a matter of choice. In practice we will usually limit ourselves to single and double excitations, and sometimes also triple excitations. It is also possible, by taking inspiration from adaptive variants of VQE [12], to pick the most relevant excitations adaptively. This is described by, and used in, Ref. [36].

Contrary to variational approaches like VQE, which aim at minimizing the parametric energy

$$E(t) = \langle \Psi(t) | \hat{H} | \Psi(t) \rangle, \qquad (3)$$

the PQE method consists in optimizing the parameters t to bring our state as close to an eigenstate as possible. This is achieved by considering an orthonormal basis $\{|\Phi_{\nu}\rangle\}$ containing $|\Phi_{0}\rangle$ (which, when $|\Phi_{0}\rangle$ is the Hartree Fock (HF) state, will correspond to excited HF determinants), and by minimizing the so-called residues:

$$r_{\nu}(\mathbf{t}) = \langle \Phi_{\nu} | \hat{U}^{\dagger}(\mathbf{t}) \hat{H} \hat{U}(\mathbf{t}) | \Phi_{0} \rangle, \qquad (4)$$

which correspond to the projection of $\hat{H} | \Psi(t) \rangle$ onto our basis (rotated by U(t)). PQE thus boils down to solving the nonlinear system of equations:

$$\forall \nu \neq 0, \ r_{\nu}(\mathbf{t}) = 0, \tag{5}$$

for $t \in \mathbb{R}^N$. This set of equations is very similar to the set of equations that is solved in the coupled cluster method in its projective, as opposed to variational, variant [4]. The main difference between PQE and projective coupled cluster is that PQE uses a unitary coupled cluster ansatz, which is efficiently implementable as a quantum circuit. At this stage, two practical implementation remarks are in order: First, since the number of possible excited states $|\Phi_{\nu}\rangle$ grows exponentially with the number of orbitals, in practice, one solves the subsystem on a subset of the possible excitations. Here, we will choose the same—possibly adaptively chosen—subset A as the one used to generate the ansatz. We will thus use the same indices μ for the residues as for the parameters. The mathematical motivations of this choice will become more apparent in section 3.

Second, in practice, the solution of this nonlinear system of equations is nontrivial. Ref. [36] advocates an approximation of a modified Newton-Raphson process. Instead of the standard Newton-Raphson strategy, which updates parameter $t^{(n)}$ at step n following

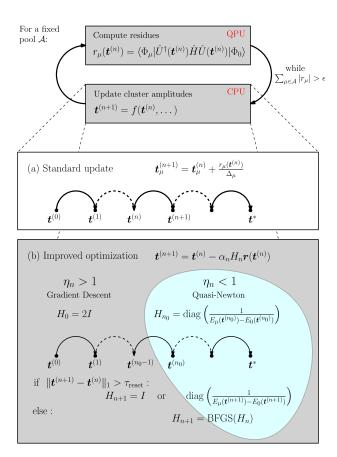


Figure 1: Outline of the projective quantum eigensolver for a fixed operator pool \mathcal{A} . The residues r_{μ} are computed using Eq. (9). Two update rules for the cluster amplitudes \boldsymbol{t} are depicted: (a) Standard update proposed in [36], with Δ_{μ} defined in Eq. (8). (b) Improved update (introduced in section 4, Algorithm 1), which (mainly) depends on the value of η_n (Eq. (46)).

the update rule

$$\mathbf{t}^{(n+1)} = \mathbf{t}^{(n)} - \mathbf{J}^{-1}(\mathbf{t}^{(n)})\mathbf{r}(\mathbf{t}^{(n)}), \tag{6}$$

the modified Newton-Raphson method replaces $J^{-1}(t^{(n)})$ with $J^{-1}(t^{(0)})$ to avoid the cost of computing and inverting the Jacobian matrix $J_{\mu\mu'}(t) = \partial r_{\mu}/\partial t_{\mu'}(t)$ at every step. (In the case of a Hartree Fock starting point, we will have $t^{(0)} = 0$). After various approximations which will be elaborated on in a later section, Ref. [36] simplifies the update rule to

$$\mathbf{t}_{\mu}^{(n+1)} = \mathbf{t}_{\mu}^{(n)} + \frac{r_{\mu}(\mathbf{t}^{(n)})}{\Delta_{\mu}},$$
 (7)

where

$$\Delta_{\mu} = \Delta_{ij...}^{ab...} = \epsilon_i + \epsilon_j + \dots - \epsilon_a - \epsilon_b - \dots$$
 (8)

is the Møller-Plesset denominator (ϵ_i is the Hartree-Fock energy corresponding to the *i*th orbital). Fig. 1 illustrates the PQE algorithm. The standard update proposed by [36] is depicted in box (a).

Each update step requires the evaluation of the residue r_{μ} . As shown in [36], it can be expressed, using the properties $\hat{\kappa}_{\mu} |\Phi_{0}\rangle = |\Phi_{\mu}\rangle$, $\hat{\kappa}_{\mu}^{2} |\Phi_{0}\rangle = -|\Phi_{0}\rangle$,

and the ensuing relation $e^{t_{\mu}\hat{\kappa}_{\mu}}|\Phi_{0}\rangle = \cos(t_{\mu})|\Phi_{0}\rangle + \sin(t_{\mu})|\Phi_{\mu}\rangle$, as

$$r_{\mu}(\mathbf{t}) = E_{\mu}^{\frac{\pi}{4}}(\mathbf{t}) - \frac{1}{2}E_{\mu}(\mathbf{t}) - \frac{1}{2}E(\mathbf{t}),$$
 (9)

where we defined:

$$E_{\mu}^{\frac{\pi}{4}}(\boldsymbol{t}) = \langle \Phi_0 | e^{-\frac{\pi}{4}\hat{\kappa}_{\mu}} \hat{U}(\boldsymbol{t})^{\dagger} \hat{H} \hat{U}(\boldsymbol{t}) e^{\frac{\pi}{4}\hat{\kappa}_{\mu}} | \Phi_0 \rangle, \quad (10)$$

$$E_{\mu}(\mathbf{t}) = \langle \Phi_{\mu} | \hat{U}(\mathbf{t})^{\dagger} \hat{H} \hat{U}(\mathbf{t}) | \Phi_{\mu} \rangle. \tag{11}$$

This means each step of optimization requires only 2N+1 measurements, where N is the size of the operator pool. This is roughly the same cost as computing a gradient via a parameter-shift rule in VQE [19, 35]. Note that one could obtain the residues using some other measurements of the same type (see for instance [27, Equation 7]).

Such a procedure was shown, in [36], to yield better convergence properties than VQE for hydrogen chains (until 10 atoms), the algorithm yielding a similar accuracy when using the same ansatz, while requiring fewer optimization steps.

In the next sections, we will introduce an error bound for the algorithm, and then focus on a mathematical study of the optimization process in order to improve it.

1.2 Summary of our results

In this work, we mainly introduce two new results.

First, in section 2, we introduce an error bound on the energy that is returned by the PQE algorithm. This endows PQE with accuracy guarantees which VQE lacks: while a small gradient norm does not guarantee any proximity to the target energy (which is why problems such as local minima and barren plateaus can arise in VQE), a small residual norm does.

The tightness of our bound is illustrated in Figure 2 for a $\rm H_4$ molecule. In this example, our bound (red curve) is systematically within less than of an order of magnitude of the true energy error (blue curve). We discuss, in the sections below, the usefulness of this bound in terms of the convergence properties of the algorithm. We also use it to design a better stopping criterion.

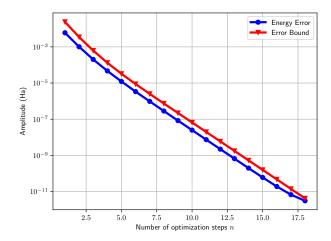


Figure 2: Test of our bound by running the PQE algorithm on an H_4 molecule at $d_{H-H}=0.8\text{Å}$ with a complete UCCSDTQ ansatz and using a convergence threshold $\epsilon=10^{-10}$. The blue slope represents the true energy error, i.e the difference $\varepsilon_{\text{exact}}(\boldsymbol{t}^{(n)})$ (defined in Eq. (19) below) between the running energy and the exact ground state energy (calculated using FCI). The red slope represents the bound on $\varepsilon_{\text{exact}}$ we derive in this work.

Our second contribution, introduced in section 4, is an optimization algorithm tailored for PQE. It switches between Newton-Raphson updates and gradient-descent-like updates based on mathematically-grounded criteria: essentially, far from the solution, updates resembling gradients descent are chosen, while approximate Newton-Raphson updates are used when closing in on the solution. This is illustrated in Fig. 1, box (b), which sketches the original PQE update rule as well as the main ideas behind our improved update rule.

A performance benchmark of our new method versus VQE and the original PQE algorithm ("Standard optimization") is presented in Fig. 3. For each of the three methods, it compares the energy error (left panels) and total number of measurements for different bond distances of the BeH₂ and LiH molecules. Two interesting features of our method stand out from this numerical comparison: it is more robust than the original PQE update rule for large bond lengths (where static correlations are larger), and much more economical than VQE (and standard PQE) in terms of the number of measurements (and hence overall run time) needed to reach a similar accuracy.

2 A general error bound for the projective quantum eigensolver

The projective quantum eigensolver computes an approximation of the ground state energy by using a simple rationale: if all the residues are zero, we are guaranteed to have an eigenvalue of the Hamiltonian. In practice, however, we will be looking at a portion of the residues, and at the end of the algorithm those

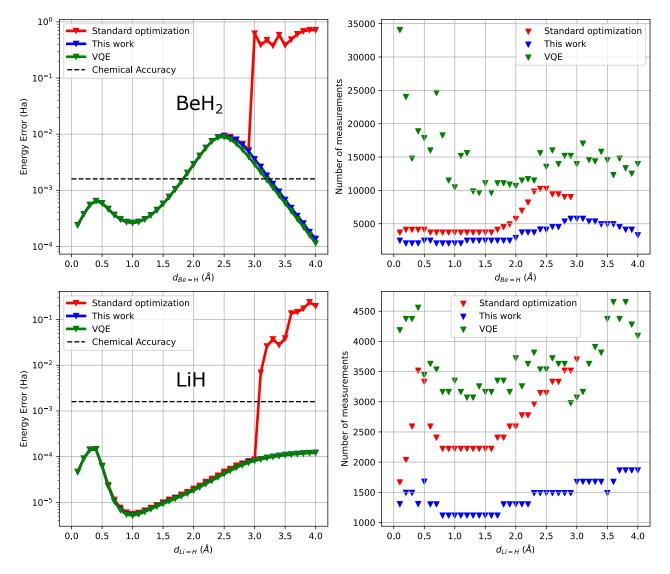


Figure 3: Comparison between the standard optimization of PQE (in red), our optimization (in blue) and VQE optimized using BFGS (in green) for computing the ground state energy of a BeH₂ (top) and LiH (bottom) molecule using a complete UCCSD ansatz at different bond distances. Left panels: energy error, i.e the difference $\varepsilon_{\rm exact}$ (see Eq. (19) below) between the energy value yielded by the algorithm and the exact FCI ground state energy computed. Right panels: total number of energy measurements (ie $\langle \Psi | \hat{H} | \Psi \rangle$ for some state $|\Psi \rangle$) performed throughout the algorithm. The x axis of each plot represents the bond distance.

will not be strictly zero, but rather smaller than a chosen threshold. It is therefore natural to wonder what guarantees on the accuracy of the result can be had by reducing residues. Moreover, the existence of such guarantees would mean that small residues imply a small error on the energy, which is not a property energy gradients in VQE have $(\vec{\nabla}E=0$ does not imply that the distance to the ground state energy vanishes).

Ref. [36] briefly mentions a bound on the error based on Gershgorin's circle theorem. In this section, we introduce a bound we have found to be much tighter, and discuss its applicability and utility.

2.1 The bound

In order to establish our bound, we introduce here Temple's inequality as presented in [14].

Theorem 1. Temple's Inequality [14, Theorem 1] Let \mathcal{H} be a self-adjoint operator on a Hilbert space with inner sesquilinear product $\langle \cdot | \cdot \rangle$. Suppose that $E_{\rm gs}$, the lowest eigenvalue of \mathcal{H} , is isolated from the rest of the spectrum ${\rm Sp}(\mathcal{H})$ and define:

$$E_{\rm es} \equiv \inf \left(\operatorname{Sp}(\mathcal{H}) \backslash \{E_{\rm gs}\} \right)$$
 (12)

Let $|\psi\rangle$ be a normalized vector of our Hilbert space such that $\langle\psi|\mathcal{H}|\psi\rangle < E_{\rm es}$. Then:

$$E_{\rm gs} \ge \langle \psi | \mathcal{H} | \psi \rangle - \frac{\langle \psi | \mathcal{H}^2 | \psi \rangle - \langle \psi | \mathcal{H} | \psi \rangle^2}{E_{\rm es} - \langle \psi | \mathcal{H} | \psi \rangle}$$
(13)

Note that the variationality of the algorithm also yields:

$$E_{\rm gs} \le \langle \psi | \mathcal{H} | \psi \rangle$$
 (14)

Namely, Temple's inequality gives us a lower bound on the energy consisting in the trial state energy minus the variance of the energy divided by an energy gap. (Note that another inequality, Kato's inequality [14, Theorem 2], is more general and could be used to obtain similar inequalities suitable for the calculation of excitation energies).

In the case of PQE, we are interested in bounding the distance between the actual ground state energy $E_{\rm gs}$ and the energy $\langle \Phi_0 | \hat{U}^{\dagger}(t) \hat{H} \hat{U}(t) | \Phi_0 \rangle$ of our trial state. We are going to apply Eq. (13) to PQE by replacing \mathcal{H} by UHU^{\dagger} and $|\psi\rangle = |\Phi_0\rangle$. With our definitions:

$$\hat{U}^{\dagger}(\boldsymbol{t})\hat{H}\hat{U}(\boldsymbol{t})|\Phi_{0}\rangle = E_{0}(\boldsymbol{t})|\Phi_{0}\rangle + \sum_{\mu} r_{\mu}(\boldsymbol{t})|\Phi_{\mu}\rangle,$$
(15)

where the sum runs on the entire (exponential in size) orthonormal basis. We thus get the numerator:

$$\langle \Phi_0 | \left(\hat{U}^{\dagger}(\boldsymbol{t}) \hat{H} \hat{U}(\boldsymbol{t}) \right)^2 | \Phi_0 \rangle -$$

$$\langle \Phi_0 | \hat{U}^{\dagger}(\boldsymbol{t}) \hat{H} \hat{U}(\boldsymbol{t}) | \Phi_0 \rangle^2 = \sum_{\mu} r_{\mu}(\boldsymbol{t})^2, \qquad (16)$$

namely the variance is given by the sum of the residues squared.

Assuming $E(t) < E_{es}$ and applying Theorem 1, we are left with the error bound:

$$E(t) - \frac{\sum_{\mu} r_{\mu}(t)^2}{E_{\text{es}} - E(t)} \le E_{\text{gs}} \le E(t)$$
 (17)

We will from now on use the notation:

$$\varepsilon_{\rm T}(t) = \frac{\sum_{\mu} r_{\mu}(t)^2}{E_{\rm es} - E(t)}.$$
 (18)

2.2 Usefulness

The error bound from Eq. (17) has a number of interesting implications.

The first one is that the smaller the term $\sum_{\mu} r_{\mu}(t)^2$, the closer we are to the ground state energy. Reducing the residues therefore makes sense in order to get a better approximation to the ground state energy. We can however expect that since there is an exponential (in the number of orbitals) amount of residues, for a given ansatz with a polynomial number of parameters, the quantity $\sum_{\mu} r_{\mu}(t)^2$ will be bounded by below, and thus so will be the best attainable accuracy.

Still, focusing on a polynomially sized set of terms \mathcal{A} is a suitable approach, provided that $\sum_{\mu \notin \mathcal{A}} r_{\mu}(t^{(0)})^2$ is small enough to allow the desired

accuracy to be reached, and provided that this quantity will not grow too much during the optimization. There is a priori no reason the second point should hold, but the reasons why it is to be expected will become clearer after section 3.

The second interesting implication of Eq. (17) is practical. During the optimization, we have access to both $\sum_{\mu \in \mathcal{A}} r_{\mu}(t)^2$ and $E_0(t)$. If we suppose that our initial state is not too bad of an approximation of the ground state, we can suppose that the initial energy $E_0(t^{(0)})$ (e.g the Hartree Fock energy) is such that $E_0(t^{(0)}) < E_{\text{es}}$ or at least $E_0(t^{(0)}) \approx E_{\text{es}}$. To shorten notation, we will from now on write $E_0 \equiv E_0(t^{(0)})$. This leads to the approximate bound:

$$\varepsilon_{\text{exact}}(t) \equiv |E(t) - E_{\text{gs}}| \le \frac{\sum_{\mu} r_{\mu}(t)^2}{E_0 - E(t)}.$$
 (19)

We are still missing $\sum_{\mu \notin \mathcal{A}} r_{\mu}(t)^2$ in order to assess the error, but as stated earlier, one can only hope that the set \mathcal{A} is good enough, such that at the start this term will be negligible with respect to the target accuracy, and that it will remain so during the optimization. Note that [36] presents a way to choose \mathcal{A} based on the residues, and that using this method makes it theoretically possible to have an estimation of $\sum_{\mu} r_{\mu}(t)^2$.

Under those assumptions, we can derive a rather well informed convergence criterion of the form:

$$\varepsilon_{\mathrm{T}}^{\mathcal{A}}(t) \equiv \frac{\sum_{\mu \in \mathcal{A}} r_{\mu}(t)^{2}}{E_{0} - E_{0}(t)} < \varepsilon$$
 (20)

where ε is a user-defined threshold.

Lastly, we would like to point out that the numerator in the rhs. of Eq. (13) corresponds to the variance of the energy. Therefore, one can see the similarity of PQE and methods such as [40] which aim at guaranteeing convergence towards an eigenstate by minimizing the variance of the energy. Here we are also interested in minimizing the variance, but only look at a portion of it. This has two upsides. The first is that looking at a carefully chosen portion of it is less costly than computing it entirely. The second one is that knowing components of the variance allows us to use them in order to reduce it, meaning we can perform advanced optimization techniques (such as the one introduced in section 4), the fast convergence of which will also help bring down the overall cost of the algorithm.

2.3 Numerical checks

2.3.1 Complete bound

In order to test the complete bound, we ran the PQE algorithm on a H₄ molecule at $d_{H-H} = 0.75\text{Å}$ using a complete UCCSDTQ ansatz. The initial state was chosen as the Hartree Fock state, which corresponds to setting $\mathbf{t}^{(0)} = 0$. Simulations were run using

our own implementation of the algorithm on Eviden's Qaptiva platform, and in particular the myQLMfermion library [13]. One and two-body integrals were computed using PySCF using a sto-3g basis. The exact values of $E_{\rm gs}$ and $E_{\rm es}$ where obtained via exact diagonalization.

The results are shown in Fig. 4. The blue slope in the following plot represents $\varepsilon_{\text{exact}}$ defined in Eq. (19) while the red and orange slopes respectively represent $\varepsilon_{\rm T}(t^{(n)})$ and $\varepsilon_{\rm T}^{\mathcal{A}}(t^{(n)})$. The green slope represents the bound mentioned in [36], which bounds the energy error with the residual 1-norm $\varepsilon_1(t) \equiv \sum_{\mu} |r_{\mu}(t)|$.

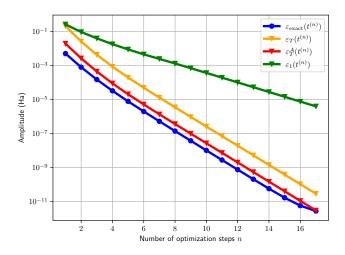


Figure 4: Comparison of the exact error $\varepsilon_{\mathrm{exact}}$, our bound ε_{T} , our more easily computable bound $\varepsilon_{\mathrm{T}}^{\mathcal{A}}$ and the bound from [36], by running the PQE algorithm on an H₄ molecule at $d_{H-H} = 0.75$ Å using a complete UCCSDTQ ansatz. The threshold for convergence ε (Eq. (20)) was set to 10^{-10} .

We can see from the simulation that our bound is about half an order of magnitude larger than the true value of the energy error, while the residual 1-norm is off by between 2 and 6 orders of magnitude. Moreover, the approximate bound provided by Eq. (19) still provides a convincing estimation of the energy error as it is off by less than 2 orders of magnitude.

2.3.2 Convergence criterion

In order to showcase the potential of the convergence criterion from Eq. (20), we ran the PQE algorithm as described in section 1.1, using different values for ε and at different bond distances d_{H-H} .

We introduce the notations:

$$\varepsilon_{\text{exact}}^* = E_0(t_{\text{final}}) - E_{\text{gs}}, \qquad (21)$$
$$\varepsilon^* = \min_{t} E_0(t) - E_{\text{gs}}, \qquad (22)$$

$$\varepsilon^* = \min E_0(t) - E_{\rm gs},\tag{22}$$

which correspond respectively to the error obtained at the end of the algorithm (and which depends on the threshold ε) and to the lowest energy error attainable within the manifold. The results are shown in Figs. 5 and 6.

For each value of d_{H-H} and ε , we plot the final value of $\varepsilon_{\mathrm{T}}^{\mathcal{A}}$ with a dashed line, and $\varepsilon_{\mathrm{exact}}^*$. The black dashed line represents ε^* , which was calculated by running VQE with the exact same UCCSD ansatz (in which second order operators are put to the right of first order ones).

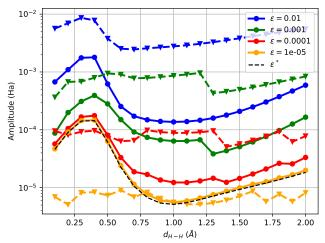


Figure 5: Test of our convergence criterion on LiH: $\varepsilon_{\rm T}$ (solid lines) and $\varepsilon_{\rm T}^{\mathcal{A}}$ (dashed lines) as a function bond distance d_{H-H} for different values of the threshold ε , with a UCCSD ansatz.

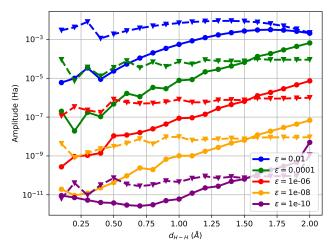


Figure 6: Same as Fig. 5 for H_4 , for a UCCSDTQ ansatz

We can see from Figure 5 that our criterion does a good job at guaranteeing a given accuracy ε when $\varepsilon^* \ll \varepsilon$. By looking at Eq. (17), one can see that the lower bound ε^* is coming from the residues which are not optimised during PQE. We would however like to point out that in highly correlated cases, there can be a slight discrepancy between the best attainable error ε^* and the error yielded by PQE with a threshold $\varepsilon \ll \varepsilon^*$. This discrepancy is explained by the fact that residues corresponding from operators not in the ansatz are slightly influenced by the choice of parameters, and thus there can be a place t^* in the

manifold, where $t^* = \arg\min_t E_0(t) - E_{\rm gs}$, such that $\varepsilon_{\rm T}^{\mathcal{A}}(t^*) \neq 0$. When looking at Figure 6, we can see that up to a value $d_{H-H} \approx 1.5 \text{Å}$, our criterion does a good job at guaranteeing a given accuracy ϵ (which can always be reached since we are using a complete ansatz). For low bond distances the discrepancy between $\varepsilon_{\rm exact}$ and $\varepsilon_{\rm T}^{\mathcal{A}}$ is rather large, while for bond distances > 1.5 Å, we no longer have $\varepsilon_{\rm exact} < \varepsilon_{\rm T}^{\mathcal{A}}$. This comes from the fact that at low bond distances, there is a large gap between $E_{\rm es}$ and the Hartree Fock energy E_0 (meaning the bound is looser), and at large bond distances $E_{\rm es} < E_0$.

3 Mathematical focus on quasi-Newton methods for PQE

Contrary to VQE where we are interested in minimizing the trial state energy, in PQE we want to find the zeros of the residue map. Common methods for approximately solving this problem are quasi-Newton methods, which will be the focus of this section. Our purpose is to introduce tools which we will later use in order to improve, both in terms of robustness and convergence speed, the optimization method proposed in [36].

3.1 On quasi-Newton methods

3.1.1 General discussion on update rules

The goal of this section is to provide the intuition leading to what will later on be properly mathematically introduced.

Given a map $F: \mathbf{t} \in \mathbb{R}^N \to F(\mathbf{t})$, the question of finding \mathbf{t}^* such that $F(\mathbf{t}^*) = 0$ is a highly nontrivial one. A common approach to such problems is the Newton-Raphson algorithm, which aims at iteratively approximately solving the root equation. Provided F is differentiable with Jacobian map J, the algorithm starts with an initial guess $\mathbf{t}^{(0)}$ and updates $\mathbf{t}^{(n)}$ following the update rule:

$$\mathbf{t}^{(n+1)} = \mathbf{t}^{(n)} - J(\mathbf{t}^{(n)})^{-1} F(\mathbf{t}^{(n)})$$
 (23)

This requires each $J(t^{(n)})$ to be non-singular.

The motivation for such an update rule is the following: suppose that for a given t one can linearly approximate $F(t + \Delta t) - F(t)$, meaning one can write $F(t + \Delta t) - F(t) \approx A(t)\Delta t$. Then if A(t) is non-singular we get for $\Delta t = -A(t)^{-1}F(t)$:

$$F(t + \Delta t) \approx F(t) - A(t)(A(t)^{-1}F(t)) = 0$$
 (24)

Therefore, if the linear approximation is good, we should expect $F(t + \Delta t)$ to be small. For $F(t + \Delta t)$ to be the smallest possible, it makes sense to use the best linear approximation of $F(t + \Delta t) - F(t)$, which for a small Δt is known to be obtained by choosing A(t) = J(t).

The quality of the update rule given by (23) is highly dependent on how well $\Delta t \to J(t)\Delta t$ approximates $F(t + \Delta t) - F(t)$.

Now, without any straightforward way to compute J(t), or if the cost of inverting it is too high, one can use an approximation A of it. Then, provided that this approximation is good enough (ie close to J(t)), then the update rule:

$$\mathbf{t}^{(n+1)} = \mathbf{t}^{(n)} - A(\mathbf{t}^{(n)})^{-1} F(\mathbf{t}^{(n)})$$
 (25)

should still perform well (provided Newton-Raphson does).

This is the idea behind the modified Newton-Raphson algorithm, which replaces $J(t)^{-1}$ with $J(t^{(0)})^{-1}$ to avoid the computational cost of computing and inverting J(t) at each step. The idea is simply that if the optimization does not go too far from $t^{(0)}$ (meaning the solution is close to the initial guess), $J(t^{(0)})$ should remain somewhat close to J(t). This yields the update rule:

$$\mathbf{t}^{(n+1)} = \mathbf{t}^{(n)} - J(\mathbf{t}^{(0)})^{-1} F(\mathbf{t}^{(n)}). \tag{26}$$

One of the caveats of the Newton-Raphson algorithm is that the Jacobian matrix J(t) is only the best linear approximation of the variations of F around t, meaning that for the algorithm to converge, an optimization step Δt should be small enough for J(t)to approximate $F(t + \Delta t) - F(t)$ well. Therefore, one might encounter cases where Δt is too big and thus $\Delta t \to F(t + \Delta t) - F(t)$ is very poorly approximated by $\Delta t \to J(t)\Delta t$. A naive workaround is to add a variable step size chosen via a line search on the norm of F. This can however lead to slow convergence in such cases, and adding a line search can make each step much more expensive computationally. In such cases, it can also be better to use a linear approximation of $\Delta t \to F(t + \Delta t) - F(t)$ which is worse around t, but will overall yield better approximations of $\Delta t \to F(t+\Delta t)-F(t)$. We will see in the next sections that such cases do exist in PQE and that there are workarounds in order to optimize the residues. Note that in what precedes we hide the subtlety induced by the fact that the size of the steps we will perform will depend heavily on the approximation we use.

The next section will introduce the Newton-Kantorovich theorem, which provides a convergence criterion for the Newton-Raphson and modified-Newton-Raphson algorithms, allowing us to have a proper mathematical framework to complete our intuition.

3.1.2 The Newton-Kantorovich theorem

First stated by Kantorovich in 1948, the Newton-Kantorovich theorem has since been refined and generalized. We here introduce the version proven in [2]:

Theorem 2 (Newton-Kantorovich Theorem). Let $t_0 \in \mathbb{R}^N$, let $F : \mathcal{B}(t_0, R) \to \mathbb{R}^N$ a Frechetdifferentiable operator, let $t \to J(t)$ its Jacobian map. Suppose:

$$J(\mathbf{t}_0) \in \mathrm{GL}_N(\mathbb{R}) \tag{27}$$

and there exists η , L > 0 such that:

$$J(\boldsymbol{t}_0)^{-1}F(\boldsymbol{t}_0) \le \eta, \tag{28}$$

For all $\mathbf{t} \in \mathcal{B}(\mathbf{t}_0, R)$, (29)

$$||J(t_0)^{(-1)}J(t)-I|| \le L||t-t_0||,$$

$$\eta L < \frac{1}{2},
\tag{30}$$

$$\frac{1 - \sqrt{1 - 2L\eta}}{L} \le R. \tag{31}$$

Then, the modified Newton-Raphson sequence defined

$$\boldsymbol{t}^{(0)} = \boldsymbol{t}_0 \tag{32}$$

$$\mathbf{t}^{(n+1)} = \mathbf{t}^{(n)} - J(\mathbf{t}_0)^{-1} F(\mathbf{t}^{(n)})$$
 (33)

converges to a unique root solution t^* of the equation F(t) = 0. Moreover, we have the following estimates for $n \geq 0$:

$$\|\mathbf{t}^{(n+1)} - \mathbf{t}^{(n)}\| \le q^n \|\mathbf{t}^{(1)} - \mathbf{t}^{(0)}\|,$$
 (34)

$$\|\boldsymbol{t}^{(n)} - \boldsymbol{t}^*\| \le \frac{q^n}{1-q} \eta = \frac{q^n}{1-q} \|\boldsymbol{t}^{(1)} - \boldsymbol{t}^{(0)}\|, \quad (35)$$

where $q = 1 - \sqrt{1 - 2\eta L}$

Additionaly, if we have:

For all
$$\mathbf{t} \in \mathcal{B}(\mathbf{t}_0, R)$$
, $J(\mathbf{t}) \in GL_N(\mathbb{R})$ (36)

Then, the Newton-Raphson sequence defined by:

$$\mathbf{t}^{(0)} = \mathbf{t}_0 \tag{37}$$

$$\mathbf{t}^{(0)} = \mathbf{t}_0$$
 (37)
 $\mathbf{t}^{(\mathbf{n}+\mathbf{1})} = \mathbf{t}^{(\mathbf{n})} - J(\mathbf{t}^{(\mathbf{n})})^{-1} F(\mathbf{t}^{(\mathbf{n})})$ (38)

converges to a unique root solution t^* of the equation F(t) = 0.

The Newton-Kantorovich Theorem provides both qualitative and quantitative insights into the Newton-Raphson and modified Newton-Raphson algorithms. Moreover, the hypotheses of the theorem properly formulate the intuitions (such as the ones we discuss in 3.1.1) one can have on quasi-Newton methods.

Theorem 2 also contains statements about convergence speed which will be the focus of subsection 3.3.

While (29) encompasses the size of the first optimization step, which can be seen as an indicator of how far from the initial guess the optimization might go wrt. how much F varies, Eq. (31) can be seen as a weaker Lipschitz-continuity condition for $t \to J(t_0)^{-1}J(t)$. Intuitively, since one wants F to be as 'linear' as possible, in which case its Jacobian map would be constant, and the constant L (which is essentially a 'weaker' Lipschitz constant) can be seen as an indicator of how constant the Jacobian map is, and therefore as an indicator of how far F is from a linear map. Mathematically, L plays a role in how contracting the update map is (the Lipschitz constant of the update map being q, see the proof of Theorem 5 in [2]). The lower L, the more contracting it is. The update map being contracting is what provides the solution existence and uniqueness, and the more contracting it is, the faster the convergence of the algorithm.

Noticing that the optimization algorithm for the PQE introduced in [36] can be seen as an approximation of a modified Newton-Raphson algorithm, one can hope to use this theorem to obtain insights into the convergence properties of the algorithm.

The next sections focus on introducing several update rules for PQE and on studying their convergence properties using the tools we have introduced.

3.2 Proof of concept: deriving a hybrid update rule

In our previous section, we introduced general formulas for quasi-Newton update rules, mainly the well known Newton-Raphson update rule (Eq. (6), and the lesser known modified-Newton-Raphson (Eq. (32)). Both update rules require knowledge on the Jacobian map of our operator, the former requiring the computation of the Jacobian matrix at each iteration while the latter only requires the Jacobian matrix at the initial point. More generally, quasi-Newton update rules require some linear approximation of the variations of our operator.

In the case of the residue map, which is the operator whose roots we want to find, computing the Jacobian matrix is however highly non-trivial. We introduce in this section two update rules aiming at approximating a Newton-Raphson and a modified-Newton-Raphson optimization. We then show that using Theorem 2, we can combine it with the update rule from [36] to obtain better convergence properties.

3.2.1 The update rules

The update rule advocated by Stair & Al. [36], Eq. (7), the derivation of which can be found in A.1, can be seen as an approximation of a modified Newton-Raphson update rule with $\mathbf{t}^{(0)} = 0$ (the starting point is the classically obtained Hartree Fock state) and with $J(0) \approx \delta_{\mu,\nu} \Delta_{\mu}$.

This latter approximation amounts to neglecting correlation terms in the Hamiltonian. One can thus see that it is possible to obtain a systematically better approximation of J(0) by taking into account correlation terms affecting the diagonal of the Hamiltonian (in other terms, by approximating \hat{H} with its entire diagonal instead of taking only a part of it). This leads to the quite similar update rule:

$$\mathbf{t}_{\mu}^{(n+1)} = \mathbf{t}_{\mu}^{(n)} + \frac{r_{\mu}(\mathbf{t}^{(n)})}{E_0(0) - E_{\mu}(0)}.$$
 (39)

In cases where the solution is fairly close to our starting point, we have found in our simulations that using this update rule yielded a better convergence rate than the rule from Eq. (7). However, this approximation results in the idea that getting a better approximation of J(0) will yield a better linear approximation of the residue map during the optimization. This is however not the case when the solution lies in a region where J(0) is a bad linear approximation. Thus, this approximation makes sense only when J(0) is overall a good linear approximation of the residue map in the region in which we are interested. For instance, in cases where correlation is strong, the solution to the residual equations lies far from the Hartree Fock state, and thus a linear approximation based on the Jacobian matrix at 0 is not good enough for convergence to take place. Intriguingly, we have found empirically that neglecting the correlation terms altogether (namely using diag $(-\delta_{\mu,\nu}\Delta_{\mu})_{\mu,\nu\in\mathcal{A}}$ in place of J(0), see 3 for more details) leads to an overall decent linear approximation of the variations in some of those cases.

If we now want to approximate a Newton-Raphson update rule (as opposed to modified Newton-Raphson), one can show (see Appendix A.1) that $J(t) \approx (E_{\mu}(t) - E_{0}(t))_{\mu,\nu \in \mathcal{A}}$, leading to the update rule:

$$\mathbf{t}_{\mu}^{(n+1)} = \mathbf{t}_{\mu}^{(n)} + \frac{r_{\mu}(\mathbf{t}^{(n)})}{E_0(\mathbf{t}^{(n)}) - E_{\mu}(\mathbf{t}^{(n)})}.$$
 (40)

Since this rule approximates J(t) instead of J(0), one can expect it to converge faster than (39). However, this update rule is still based on the assumption that the solution will not be too far from the starting point, and thus the Jacobian map will yield a good linear approximation of the variations of the residue map close to the solution, which is not always the region of interest. We will show in section 3.2.3 that the update rule from Eq. (7) yields better stability than this one.

Following the convergence properties of both the update rules from Eq. (7) and Eq. (40), it is only natural to want to combine the good properties of both, mainly:

- The higher convergence speed of the approximate Newton-Raphson update rule
- The better stability of the standard update rule.

The next subsection is devoted to using Theorem (2) in order to obtain an update rule combining both.

3.2.2 Deriving the hybrid update rule

We discussed in section 3.1.1 three update rules, the two of interest being the approximate Newton-Raphson update rule (Eq. (40)), and the standard update rule (Eq. (7)), the pros and cons of which can be summarized as:

- An approximation of a Newton-Raphson (40) optimization is faster than the standard update rule (7) when it converges.
- The standard update rule converges in more cases.

One can show (see Appendix A.1) that we have the approximate inequality for t_1 , $t_2 \ll 1$:

$$||J(t_1)^{-1}(J(t_2) - J(t_1)||_1 \le ||t_1 - t_2||_1.$$
 (41)

This means that the constant L is approximately equal to 1. In turn, this implies the convergence condition (30) from Theorem 2 now reads:

$$\eta < \frac{1}{2}
\tag{42}$$

i.e
$$||J(\mathbf{t}^{(0)})^{-1}r(\mathbf{t}^{(0)})||_1 < \frac{1}{2}$$
 (43)

Therefore, we can approximately predict when a Newton-Raphson optimization will converge by looking at the 1-norm of the first optimization step. In the context of the approximate Newton-Raphson update rule, this reads:

$$\sum_{\mu \in \mathcal{A}} \left| \frac{r_{\mu}(\mathbf{t}^{(0)})}{E_{\mu}(\mathbf{t}^{(0)}) - E_{0}(\mathbf{t}^{(0)})} \right| < \frac{1}{2}$$
 (44)

It thus seems natural to use this criterion to select the best update rule at each step: we start the optimization using (7) until the convergence criterion is met (ie we are close enough to the solution), and then to take advantage of the faster convergence of (40).

This leads to the update rule which we dub 'hybrid':

$$\mathbf{t}_{\mu}^{(n+1)} = \begin{cases} t_{\mu}^{(n)} + \frac{r_{\mu}(\mathbf{t}^{(n)})}{\Delta_{\mu}} & \text{if } \eta_{n} > \frac{1}{2} \\ t_{\mu}^{(n)} + \frac{r_{\mu}(\mathbf{t}^{(n)})}{E_{0}(\mathbf{t}^{(n)}) - E_{\mu}(\mathbf{t}^{(n)})} & \text{otherwise} \end{cases}$$
(45)

where:

$$\eta_n \equiv \left\| \left(\frac{r_{\mu}(\mathbf{t}^{(n)})}{E_{\mu}(\mathbf{t}^{(n)}) - E_0(\mathbf{t}^{(n)})} \right)_{\mu \in \mathcal{A}} \right\|_1. \tag{46}$$

We will show in the next section that this update rule allows a faster convergence of the residues and is slightly more robust than the standard update rule (7).

3.2.3 Benchmarks and discussion

To compare the different optimization methods, we ran the algorithm using each method on Eviden's Qaptiva simulation platform, on H₄, H₆, and BeH₂ molecules corresponding to 8, 12 and 14 qubits, respectively, for bond distances ranging from 0.1Å to 4Å. Hartree Fock calculations and one and two-body integral calculations where performed using PySCF with a sto-3g basis. The translation from fermionic to spin operators was performed using the Jordan-Wigner encoding [16]. We use the exact same UCCSD ansatz for each optimization method, in which the ordering reads $\hat{U}(t) = \hat{U}_1(t)\hat{U}_2(t)$ where \hat{U}_1 contains the first order excitation operators, and \hat{U}_2 contains the second order excitation operators. We use a convergence threshold $\varepsilon = 10^{-5}$ (as defined in Eq. (20)), and as usual a starting point $t^{(0)} = 0$.

We introduce two notations for simplicity: $\varepsilon_{\rm final}$ refers to the energy after convergence, while ε^* refers to the lowest energy encountered during the algorithm.

When looking at Figure 7, we can see that the hybrid update rule performs better on H_4 than the standard update rule: it requires systematically fewer steps for convergence, and while the standard update rule stops converging around 2Å, the hybrid update rule converges until 2.8Å. As expected, the approximate Newton-Raphson update rule performs similarly to the hybrid update rule at low bond distances, but becomes worse between 1Å and 1.6Å, and even though it is then slightly better then, it stops converging sooner, around 2.2Å. This suggest that perhaps the threshold for the switch between the standard update rule and the approximate Newton-Raphson update rule could be increased, meaning the approximation $L \approx 1$ might be a bit of an overestimation.

On H_6 (Figure 7), we can see the same behavior: the hybrid update rule converges slightly faster than the standard one, and converges in more cases. The approximate Newton-Raphson update rule performs mostly worse than the hybrid update rule, and in some cases worse than the standard update rule.

Finally, on BeH₂ (Figure 7) we get the same behavior: the hybrid update rule is superior to the standard update rule. Again, the approximate Newton-Raphson update rule is mostly inferior to the hybrid update rule, but performs better in some cases, suggesting again that the value taken for L could be lower (ie we could switch to the approximate Newton-Raphson update rule sooner). Note that there are two points where the approximate Newton-Raphson update rule converges but not the other ones. This can be explained by the fact that the initial point is slightly good enough for a Newton-Raphson to converge, but $\eta > \frac{1}{2}$ (again, this suggests the threshold $\frac{1}{2}$ might be too conservative) and the Hartree Fock Hamiltonian approximates very poorly the Hamiltonian, and thus the standard update rule performs poorly meaning the first steps of the hybrid optimization will not bring us closer to the solution and thus the approximate Newton-Raphson part of the optimization will never start.

3.3 Proof of concept 2: convergence rate predictions

3.3.1 The Theory

Here, we wish to use the Newton Kantorovich Theorem in order to investigate the convergence of a modified Newton-Raphson optimization. We have previously introduced the update rule corresponding to an approximation of a modified Newton-Raphson optimization (see Eq. (39)), and as stated previously, using derivations found in Appendix A.1, we show that in first order in t and $t^{(0)}$, one gets:

$$||J(\mathbf{t}^{(0)})^{-1}J(\mathbf{t}) - I||_1 \le ||\mathbf{t}^{(0)} - \mathbf{t}||_1$$
 (47)

where for conciseness, $\|\cdot\|_1$ is either the 1-norm on \mathbb{R}^N or the associated operator norm.

This allows us to use Eq. (34) from Theorem 2 in order to assess the convergence rate q which, as we recall, is defined by:

$$q = 1 - \sqrt{1 - 2\eta} \tag{48}$$

and is such that:

$$\|\boldsymbol{t}^{(n)} - \boldsymbol{t}^*\| \le \frac{q^n}{1 - q} \eta,\tag{49}$$

We recall that η can be calculated as:

$$\eta \equiv \|\boldsymbol{t}^{(1)} - \boldsymbol{t}^{(0)}\|_{1} = \sum_{\mu \in \mathcal{A}} \left| \frac{r_{\mu}(\boldsymbol{t}^{(0)})}{E_{\mu}(\boldsymbol{t}^{(0)}) - E_{0}(\boldsymbol{t}^{(0)})} \right|$$
(50)

Note that if we look at (50), we can see that if $E_{\mu}(t) - E_0(t)$ is not too far from the gap between the actual ground state and the excited state corresponding to μ , then one can write:

$$q \le 1 - \sqrt{1 - 2\frac{\|r(t^{(0)})\|_1}{\Delta}}$$
 (51)

where $\Delta = E_{\rm es} - E_{\rm gs}$ is the Highest Occupied Molecular Orbital - Lowest Unoccupied Molecular Orbital (HOMO-LUMO) gap of the molecule. What we can see from Eq. (51) is that q is upper-bounded by an increasing function of the ratio between the 1-norm of $r(t^{(0)})$ and the HOMO-LUMO gap of the molecule. This also means, if we consider a fixed $||r(t^{(0)})||_1$, that a larger gap should lead to faster convergence.

3.3.2 Numerical checks

In order to check what we have been discussing, we ran simulations of the PQE algorithm using the approximate modified Newton-Raphson optimization

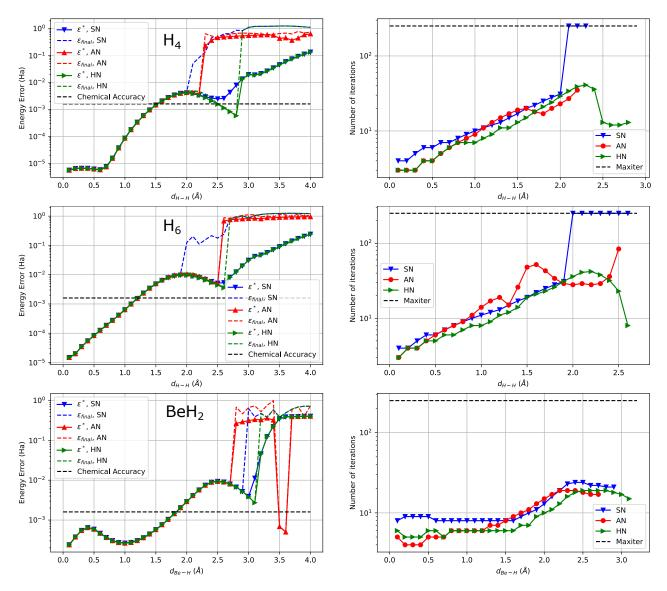


Figure 7: Comparison of the 'hybrid' quasi-Newton optimizer, the approximate Newton-Raphson optimizer, and the standard quasi-Newton optimizer for PQE ran on three molecules at different bond distances: H_4 (top), H_6 (middle) and BeH_2 (bottom). Left panels: energy error, ie the difference between the energy value yielded by the algorithm and the exact ground state energy computed via FCI. Right panels: total number of optimization steps required to reach convergence. The x axis of each plot represents the bond distance.

(Eq. (32)). According to Eq. (49), the slope of $\|\boldsymbol{t}^{(n)} - \boldsymbol{t}^{\text{final}}\|_1$ in logplot should be close to a linear plot with a slope $-\gamma = \log(q)$. We thus fit this evolution in order to obtain the coefficient γ . We also retrieve at the beginning of the algorithm the quantity η defined in (46) allowing us to obtain the lower bound of the coefficient γ :

$$\gamma_{\rm lb} = -\log(1 - \sqrt{1 - 2\eta}) \tag{52}$$

We plot γ and γ_{1b} in Figure 8 for H_4 (green slopes), H_6 (blue slopes) and BeH_2 (red slopes) molecules for different bond distances. We can see that in the case of H_4 (green slopes), our predictions get very close to the actual value while being lower (as expected). We can however see that at larger bond distances the discrepancy becomes larger: we predict a convergence

up to 0.8Å while the algorithm converges up to 1.2Å. This suggests that at higher bond distances (which in the case of H₄ means parameter vectors with larger norms) the approximation $L \approx 1$ might be an overestimation. Looking at the slopes for H₆ (blue slopes), we still get a lower bound reproducing nicely the tendency. The predictions are however far from the true value and this again gets worse with larger bond distances, suggesting again that the true value of L might be smaller than 1. In the case of BeH₂, although we still technically get a lower bound, we only predict convergence for a fraction of the cases where it does converge. Again, this can be explained by the fact that the value $L \approx 1$ might be too large. In the cases where we do not predict convergence, one can check that the norm of the parameter vectors gets to around

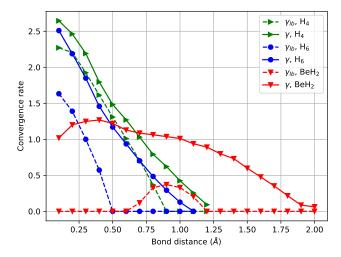


Figure 8: Actual convergence rate γ (solid lines) and predicted convergence rate $\gamma_{\rm lb}$ of the approximate modified-Newton-Raphson optimizer (Eq. (32)) in the case of H₄ (in blue), H₆ (in green) and BeH₂ (in red) molecules for several bond distances.

0.7, meaning the assumptions we used to obtain $L \approx 1$ no longer hold, hence the poor predictions. Still, we can see that our derivations do not provide very accurate quantitative predictions but are still interesting for qualitative predictions.

4 A Resource-Efficient and Robust Optimization

4.1 The Method

We have seen in the previous section that it is possible to use the Newton Kantorovich Theorem in order to obtain predictions for quasi-Newton optimizations. Still, even though our hybrid update rule displays better convergence properties, it does not converge in every case, and it is based solely on the empirical observation that the standard update rule converges in many cases.

We would like to use the idea of the hybrid optimization, which consists in using a first optimization to get to a point in the manifold where we know a Newton-Raphson optimization will converge, and then using an approximate Newton-Raphson to take advantage of its faster convergence. Previously, we used the standard optimization (Eq. (7)) to get to the point in question, but it does not work in every case. The first idea of our novel optimization method is the following: gradient descents on the energy have the upside of not requiring that the starting point in parameter space be close to the converged parameter. Moreover, since we are in the end interested in the energy, making sure we reduce it each step makes sense.

Finally, one can check that (see appendix A.1):

$$\frac{\partial E_0}{\partial t_{\mu}}(\mathbf{t}) = 2r_{\mu}(\mathbf{t}) + O(\|\mathbf{t}\|). \tag{53}$$

This means that instead of following the gradient at a given point to get an improvement on the energy, one can follow the residues, the upside being that we can check at each step whether a Newton-Raphson will converge, and we can still use the well-informed convergence criterion from Eq. (20). This also means that as long as we are far from the solution, the residues should remain big, meaning there will not be any barren plateau or local minima phenomenon. One could argue that in cases where the gradients are small but the residues are not (which means Eq. (53) is a poor approximation), there is no real reason that the direction given by the residue vector should yield improvements on the energy. This difficulty should be somewhat alleviated by the next additions, and if such cases arise one could always replace this step with another residue-based scheme.

This first idea thus gives rise to the following update rule:

$$\boldsymbol{t}_{\mu}^{(n+1)} = \begin{cases} & \boldsymbol{t}_{\mu}^{(n)} - 2r_{\mu}(\boldsymbol{t}^{(n)}) \text{ if } \eta_{n} > \frac{1}{2L} \\ & \boldsymbol{t}_{\mu}^{(n)} - \frac{r_{\mu}(\boldsymbol{t}^{(n)})}{E_{\mu}(\boldsymbol{t}^{(n)}) - E_{0}(\boldsymbol{t}^{(n)})} \text{ otherwise} \end{cases},$$
(54)

where L is the constant from Theorem 2. The goal of the first update rule is thus solely to bring us to a place in the manifold where $\eta_n < \frac{1}{2L}$.

Since we are primarily interested in cases where t^* is far from $t^{(0)}$, we however expect the difference in direction between the gradients and the residues to be non negligible, and vanilla gradient descent with a learning rate of 1 lacks robustness, we add a variable step size α_n such that:

$$\boldsymbol{t}_{\mu}^{(n+1)} = \begin{cases} & \boldsymbol{t}_{\mu}^{(n)} - 2\alpha_{n}r_{\mu}(\boldsymbol{t}^{(n)}) \text{ if } \eta_{n} > \frac{1}{2L} \\ & \boldsymbol{t}_{\mu}^{(n)} - \frac{r_{\mu}(\boldsymbol{t}^{(n)})}{E_{\mu}(\boldsymbol{t}^{(n)}) - E_{0}(\boldsymbol{t}^{(n)})} \text{ otherwise} \end{cases}$$
(55)

 α_n is chosen using a backtracking line search on the energy and such that it respects the Armijo condition for a parameter c < 1 (for more details, read [30, sections 3.1 and 3.2]). If such an α_n is not found (or rather is below a user-defined threshold $\alpha_{\rm threshold}$, such as $\alpha_{\rm threshold} = 10^{-10}$), the algorithm terminates.

We could enforce the Wolfe condition [30], i.e add a curvature condition, but since measuring the residues is much more costly than just measuring the energy, and the residues are not really equal to the gradients, we simply choose to forego the curvature condition. Moreover, the curvature is not needed when using a backtracking line search for Newton methods.

Since this line search is fairly cheap in comparison with each optimization step, we also add a variable step length to the quasi-Newton part of the optimization in order to make it more robust. The line search is therefore performed in each case, after determining which update rule to use. We are left with the update rule:

$$\boldsymbol{t}_{\mu}^{(n+1)} = \begin{cases} \boldsymbol{t}_{\mu}^{(n)} - 2\alpha_{n}r_{\mu}(\boldsymbol{t}^{(n)}) & \text{if } \eta_{n} > \frac{1}{2L} \\ \boldsymbol{t}_{\mu}^{(n)} - \alpha_{n} \frac{r_{\mu}(\boldsymbol{t}^{(n)})}{E_{\mu}(\boldsymbol{t}^{(n)}) - E_{0}(\boldsymbol{t}^{(n)})} & \text{otherwise} \end{cases}$$

$$(56)$$

The last idea of our optimization method is to take advantage of the curvature information we have gathered during the previous iterations using the BFGS update rule ([30]). The BFGS algorithm uses curvature information from past iterations in order to iteratively construct an approximation of the Hessian of the cost function. In our case, we are interested in improving our guess of inverse Jacobian since we are using an approximation which can be fairly rough in highly correlated cases.

We therefore introduce the update rule:

$$\mathbf{t}^{(n+1)} = \mathbf{t}^{(n)} - \alpha_n H_n r(\mathbf{t}^{(n)}),$$
 (57)

where H_n will be updated using the BFGS update rule:

$$H_{n+1} = H_n + \frac{\left(s_n^T y_n + y_n^T H_n y_n\right) \left(s_n s_n^T\right)}{\left(s_n^T y_n\right)^2} - \frac{H_n y_n s_n^T + s_n y_n^T H_n}{s_n^T y_n}$$
(58)

where $y_n = r(\mathbf{t}^{(n+1)}) - r(\mathbf{t}^{(n)})$ and $s_n - \alpha_n H_n r(\mathbf{t}^{(n)})$.

We also use the tools we have derived so far. Namely, we start with $H_0 = 2I$ or $H_0 =$ diag $\left(\left(\frac{1}{E_{\mu}(t^{(0)})-E_{0}(t^{(0)})}\right)_{\mu\in\mathcal{A}}\right)$ depending on the value of η wrt. a user-defined threshold $\eta_{\text{threshold}}$. Typically, we have seen that a threshold $\eta_{\text{threshold}} = \frac{1}{2}$ works well, but since we can see from section 3.3.2 that the value $L \approx 1$ can be an overestimation, and since the line search makes everything more robust, the threshold can be increased. We have found that a threshold $\eta_{\text{threshold}} = 1$ typically works well.

During the optimization, if we started with $H_0 =$ 2I, we test at each step whether the criterion is met, and if it is at step n, then we use $H_{n+1} =$ diag $\left(\left(\frac{1}{E_{\mu}(\boldsymbol{t}^{(n)})-E_{0}(\boldsymbol{t}^{(n)})}\right)_{n\in\Lambda}\right)$.

```
Algorithm 1 Our Optimization Method
  1: Input: Starting point t^{(0)}, onvergence thresh-
       old \varepsilon, switch threshold \eta_{\rm threshold} (typically 1), re-
       set threshold \tau_{\rm reset} (typically \frac{1}{2}), Armijo threshold c (typically 10^{-4}), linesearch stop threshold
       \alpha_{\rm threshold} (typically 10^{-10}).
  2: Compute E_0(\mathbf{t}^{(0)}) and the values (r_{\mu}(\mathbf{t}^{(0)}))_{\mu \in \mathcal{A}},
       (E_{\mu}(\boldsymbol{t}^{(0)}))_{\mu \in \mathcal{A}}.
  4: Compute \eta_0 = \sum_{\mu \in \mathcal{A}} \left| \frac{r_{\mu}(\boldsymbol{t}^{(0)})}{E_{\mu}(\boldsymbol{t}^{(0)}) - E_0(\boldsymbol{t}^{(0)})} \right|
  5: if \eta_0 < \eta_{\rm threshold} then
                    H_0 = \operatorname{diag}\left(\frac{1}{(E_u(\boldsymbol{t}^{(0)}) - E_0(\boldsymbol{t}^{(0)}))}\right)
  7: else: H_0 = 2I
  8: end if
  9: while \epsilon_{\mathrm{T}}^{\mathcal{A}}(\boldsymbol{t}^{(n)}) > \epsilon \ \mathbf{do}
              Backtracking line search: Find step size \alpha_n
       such that:
       E_0\left(\boldsymbol{t}^{(n)} - \alpha_n H_n r(\boldsymbol{t}^{(n)})\right) < E(\boldsymbol{t}^{(n)}) - c \cdot \alpha_n (H_n r(\boldsymbol{t}^{(n)}))^T r(\boldsymbol{t}^{(n)})
              if \alpha < \alpha_{\rm threshold} then
11:
                     Return t^{(n)}, E_0(t^{(n)})
12:
              end if
13:
              Update parameter: t^{(n+1)} = t^{(n)} –
14:
       \alpha_n H_n r(\boldsymbol{t}^{(n)})
              Compute r(\boldsymbol{t}^{(n+1)}), (E_{\mu}(\boldsymbol{t}^{(n+1)}))_{\mu \in A}
15:
              Compute \eta_{n+1}
16:
17:
              Compute
                 \epsilon_{\mathrm{T}}^{\mathcal{A}}(\boldsymbol{t}^{(n+1)}) = \sum_{\boldsymbol{x} \in \mathcal{A}} \frac{r_{\mu}(\boldsymbol{t}^{(n+1)})^{2}}{E_{0}(\boldsymbol{t}^{(0)}) - E_{0}(\boldsymbol{t}^{(n+1)})}
              if \eta_{n+1} < \eta_{\text{threshold}} and \eta_n > \eta_{\text{threshold}} then
18:
                     Set H_{n+1} = \text{diag}\left(\frac{1}{(E_u(\mathbf{t}^{(n+1)}) - E_0(\mathbf{t}^{(n+1)}))}\right)
19:
20:
                     if \|\boldsymbol{t}^{(n+1)} - \boldsymbol{t}^{(n)}\|_1 > \tau_{\text{reset}} then
21:
22:
                            if \eta_{n+1} < \eta_{\text{threshold}} then
23:
                 H_{n+1} = \operatorname{diag}\left(\frac{1}{\left(E_{u}(\boldsymbol{t}^{(n+1)}) - E_{0}(\boldsymbol{t}^{(n+1)})\right)}\right)
24:
                            else
                                   Set
25:
                                              H_{n+1} = 2I
                            end if
26:
                     else
27:
                            Update inverse Jacobian guess:
```

29:

30:

Eq. (58)

31: end while

end if

end if

32: **Return** $t^{(n+1)}$, $E_0(t^{(n+1)})$

A last improvement which is less important but makes sense, is that since we are dealing with optimizations that might go far from the starting point, and with manifolds which typically are not close to linear (otherwise we would use a quasi-Newton from the start), we choose to discard curvature information from previous iterations if the current parameter is far from the previous one. That is, if $\|\mathbf{t}^{(n+1)} - \mathbf{t}^{(n)}\|_1 > \tau_{\text{reset}}$ we use $H_{n+1} = 2I$ or $H_{n+1} = \text{diag}\left(\left(\frac{1}{E_{\mu}(\mathbf{t}^{(n+1)}) - E_0(\mathbf{t}^{(n+1)})}\right)_{\mu \in \mathcal{A}}\right)$ depending on the value of η_n . τ_{reset} is chosen by the user, but we have found that $\tau_{\text{reset}} = \frac{1}{2}$ works fairly well (notice that this value makes sense wrt. our study so far). Lastly, we would like to point out that foregoing the curvature condition during the line search means there theoretically might be cases where H_n is not positive-definite. Although we have not encountered this case, one can simply choose not to update H_n if the update would make it non-positive-definite. Since the BFGS update rule is really not a central point of our method (its purpose is just to make our approximation of the Jacobian a bit better), it is reasonable to do so.

The pseudocode of the algorithm is available under Algorithm 1.

4.2 Benchmarks

In order to test our optimization, we ran our implementation of it on Eviden's Qaptiva platform, for H₄, H₆, LiH and BeH₂ molecules using the same ansatz as mentioned in subsection 3.2.3. We used the same threshold $\varepsilon = 10^{-5}$ for both the standard optimization and our optimization. We also ran our implementation of the variational quantum eigensolver, again with the same ansatz, where the parameters t were optimized using the implementation of BFGS provided by ScipyMinimize with a threshold for the gradient norm of 10^{-5} . In order to compare the algorithms, we plot the difference between the converged energy and the energy computed using FCI (ran using PySCF) which we dub the energy error, and we plot the total number of energy measurements used by the algorithm. The results can be found in Figures 3, 10 and 9.

We can see when looking at Fig. 3 that PQE (both using the standard optimization and our optimization) performs comparably to VQE in terms of energy error for bond distances smaller than 3 Å. Beyond that, the standard optimization stops converging while ours still does. The results obtained are still quite comparable to VQE, although there is a slight discrepancy, the origin of which has been discussed in subsection 2.3.2. In terms of number of measurements however, we can see that our algorithm beats both VQE and the standard implementation of PQE.

The same can be said when looking at LiH (Fig.

3): PQE with our optimization yields results comparable with that of VQE, but does so with far less measurements than both VQE and the standard implementation of PQE, which does not converge past 3 Å.

In the cases of Hydrogen chains H_4 and H_6 (Figures 9 and 10), the standard implementation of PQE quickly gets worse than VQE in terms of number of energy measurements, and stops converging for bond distances larger than 2 Å. Our optimization however, converges in every case, and yields comparable results to VQE accuracy-wise, while being mostly superior measurements-wise. The cases where our algorithm takes a bit more measurements correspond to cases where the global minimum of the energy is in a place of the landscape where the convergence criterion is not met, therefore the algorithm performs a few superfluous steps without being able to get much improvement on the residual norm, and then stops when the line search yields steps too small.

Overall, our method yields results comparable to the ones given by VQE, while requiring in most cases far fewer energy measurements and offering the theoretical guarantees we have previously discussed.

5 Conclusion

In this work, we have shown evidence of promising aspects of residue-based optimizations for unitary coupled cluster calculations on quantum processors. These promising aspects include robust convergence properties when getting close enough to the solution. These convergence features are similar to the ones which can be obtained with the variance-based variational quantum eigensolver [40], albeit without the additional computational overhead. We anticipate that these convergence properties could potentially at least partially solve some of the challenges encountered with the standard VQE approach, such as barren plateaus and local minima. We have also shown, using our novel optimization method, that such methods can more than rival the variational quantum eigensolver in terms of computational cost. However, our method still faces challenges in the same capacity as VQE, mainly measurement overhead and noise sensitivity for NISQ computations, which means that even with better hardware, more algorithmic improvements will be needed in order to obtain a viable alternative to classically computed coupled cluster, or an efficient state preparation method for quantum phase estimation.

Acknowledgements

This work was supported by the ANR Research Collaborative Project 'QuRes' (Grant ANR-PRC-CES47-0019). As part of the MetriQs-France pro-

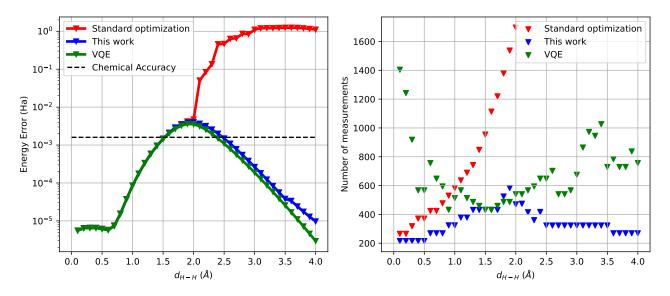


Figure 9: Same as Fig. 3 but on a H₄ molecule

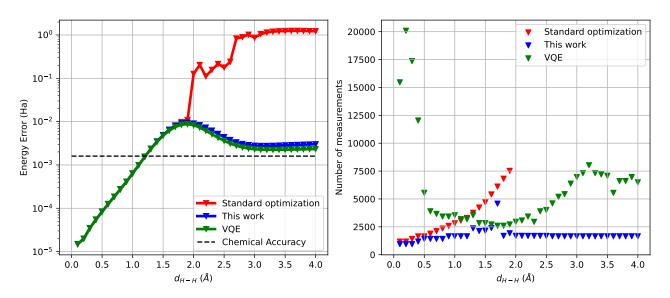


Figure 10: Same as Fig. 3 but on a H_6 molecule

gram, this work was supported by France 2030 under the French National Research Agency grant number ANR-22-QMET-0002. As part of the HQI initiative, this work was supported by France 2030 under the French National Research Agency award number ANR-22-PNCQ-0002. The authors thank Alexia Auffèves for her involvement in making this work possible. The authors also acknowledge useful discussions with Cyrielle Martin, Mohammad Hassan, Robert Whitney and Victor Kadri. The computations were performed on the Eviden Qaptiva platform.

A Mathematical derivations

A.1 Jacobian map approximations

In this subsection, we present the calculations and approximations allowing us to obtain the approximate Newton-Raphson and approximate modified-Newton-Raphson update rules (Eq. (40) and (39)). The main assumption here will be that the Hartree Fock approximation is already a good step towards computing the ground state. This will lead to our two main assumptions. The first one is the assumption that the Hamiltonian written in the Hartree Fock basis (molecular orbitals) is already close to being diagonal, and that it will remain so on the rotated basis (i.e, transformed by $\hat{U}(t)$) during the optimization.

Mathematically speaking, we consider:

$$|\langle \Phi_{\mu}|\hat{U}^{\dagger}(\boldsymbol{t})\hat{H}\hat{U}(\boldsymbol{t})|\Phi_{\nu}\rangle| \ll 1$$
 (59)

for all t and $\nu \neq \mu$. Note that this implies that the quasi-Newton update rules we derive will be of order 1 in off-diagonal coefficients of the Hamiltonian. We will also assume the solution t^* of the PQE equations to be small in norm.

In what follows, we suppose a fixed parametric ansatz $\mathbf{t} \to \hat{U}(\mathbf{t}) = \prod_{\mu \in \mathcal{A}} e^{t_{\mu} \hat{\kappa}_{\mu}}$ and introduce a partial order on \mathcal{A} : $\mu > \nu$ iff $\hat{U} = \cdots e^{t_{\nu} \hat{\kappa}_{\nu}} \cdots e^{t_{\mu} \hat{\kappa}_{\mu}} \cdots$. We also introduce the notation $\mathbf{t} \to \hat{\mathcal{U}}_{\nu}(\mathbf{t}) = \prod_{\nu' > \nu} e^{t_{\nu} \hat{\kappa}_{\nu}}$. It will be assumed that indices μ, ν are in $\hat{\mathcal{A}}$ unless specified otherwise.

We recall the Baker-Campbell-Hausdorff (BCH) expansion: given two operators X and Y, one can write:

$$e^{Y}Xe^{-Y} = X + [X,Y] + \frac{1}{2}[[X,Y],Y] + \cdots$$
 (60)

In order to obtain a general formula for the Jacobian map $t \to J(t)$ of the residue map, we expand $r_{\mu}(t + \Delta t)$ and identify the coefficients of J(t) as the coefficients of the first order terms. Thus we expand $\hat{U}(t + \Delta t)^{\dagger} \hat{H} \hat{U}(t + \Delta t)$ to first order in Δt using BCH. One can easily check that we get:

$$J_{\mu,\nu}(\boldsymbol{t}) = \langle \Phi_{\mu} | \left[\hat{U}(\boldsymbol{t})^{\dagger} \hat{H} \hat{U}(\boldsymbol{t}), \hat{\mathcal{U}}_{\nu}(\boldsymbol{t})^{\dagger} \hat{\kappa}_{\nu} \hat{\mathcal{U}}_{\nu}(\boldsymbol{t}) \right] | \Phi_{0} \rangle$$

$$(61)$$

For t = 0, we simply get:

$$J_{\mu,\nu}(0) = \langle \Phi_{\mu} | \left[\hat{H}, \hat{\kappa}_{\nu} \right] | \Phi_{0} \rangle. \tag{62}$$

If, in addition, we further approximate \hat{H} with its diagonal, we get:

$$J(0)_{\mu,\nu} = \delta_{\mu,\nu} \left(E_{\mu}(0) - E_{0}(0) \right), \tag{63}$$

with $E_{\mu}(0)$ and $E_{0}(0)$ defined in the main text, Eq. (11). This approximation is what yields the approximate modified-Newton-Raphson rule introduced in Eq. (39).

Another way to approximate Eq. (62) is to consider that \hat{H} is composed of the Hartree Fock Hamiltonian $H_{HF} = \sum_{p} \epsilon_{p} \hat{a}_{p}^{\dagger} \hat{a}_{p}$ and a perturbation \hat{F} containing all the correlation terms of \hat{H} . This corresponds in Eq. (1) to $h_{pq} = \delta_{p,q} \epsilon_{p}$

This yields the approximation:

$$J(0)_{\mu,\nu} = -\delta_{\mu,\nu} \Delta_{\mu},\tag{64}$$

where $\Delta_{\mu} = \epsilon_i + \epsilon_i + \cdots - \epsilon_a - \epsilon_b - \cdots$ is the standard Møller Plesset denominator corresponding to the excitation μ . This approximation is what leads to the update rule in Eq. (7) which is introduced in [36].

Now going back to J(t), using Eq. (61) and approximating $\hat{U}(t)^{\dagger}\hat{H}\hat{U}(t)$ with its diagonal diag $(E_{\mu}(t))$ we get:

$$J_{\mu,\nu}(\mathbf{t}) = (E_{\mu}(\mathbf{t}) - E_{0}(\mathbf{t})) \langle \Phi_{\mu} | \hat{\mathcal{U}}_{\nu}^{\dagger}(\mathbf{t}) \hat{\kappa}_{\nu} \hat{\mathcal{U}}_{\nu}(\mathbf{t}) | \Phi_{0} \rangle.$$
(65)

Looking at the case $\nu \neq \mu$, we can expand $\langle \Phi_{\mu} | \hat{\mathcal{U}}_{\nu}^{\dagger}(t) \hat{\kappa}_{\nu} \hat{\mathcal{U}}_{\nu}(t) | \Phi_{0} \rangle$ using BCH:

$$\langle \Phi_{\mu} | \hat{\mathcal{U}}_{\nu}^{\dagger}(\boldsymbol{t}) \hat{\kappa}_{\nu} \hat{\mathcal{U}}_{\nu}(\boldsymbol{t}) | \Phi_{0} \rangle = \langle \Phi_{\mu} | \hat{\kappa}_{\nu} | \Phi_{0} \rangle + \sum_{\nu' > \nu} t_{\nu'} \langle \Phi_{\mu} | [\hat{\kappa}_{\nu}, \hat{\kappa}_{\nu'}] | \Phi_{0} \rangle + o(\|\boldsymbol{t}\|), \qquad (66)$$

where the term $o(\|\boldsymbol{t}\|)$ also contains higher-order commutators. When $\nu \neq \mu$ we have $\langle \Phi_{\mu} | \hat{\kappa}_{\nu} | \Phi_{0} \rangle = 0$. We then choose to neglect the other terms, considering that in cases with a low correlation the Hartree Fock state will be good enough to assume $\|t\|_{1} \ll 1$, and that even in more correlated cases most of the commutators will be zero. If $\mu = \nu$, then we get $\langle \Phi_{\mu} | \hat{\kappa}_{\nu} | \Phi_{0} \rangle = 1$, and we will neglect the other terms of the expansion for the aforementioned reasons.

We end up with the following approximation:

$$J_{\mu,\nu}(\mathbf{t}) = \delta_{\mu,\nu} \left(E_{\mu}(\mathbf{t}) - E_{0}(\mathbf{t}) \right), \tag{67}$$

which allows us to derive the update rule introduced in Eq. (40).

A.2 The constant L

The goal here is to find L such that $\|J^{-1}(J(t)-J(t^{(0)}))\| \leq L\|t\|$ (where $t^{(0)}$ is not necessarily 0 since we sometimes perform a few iterations from another method beforehand) so that we can use the Newton-Kantorovich Theorem to predict the convergence properties of the algorithm. We first go back to Eq. (65). Our goal is to use its first order in t expansion. We first notice that using BCH we get:

$$E_{\mu}(\boldsymbol{t}) = E_{\mu}(0) + \sum_{\nu \in \mathcal{A}} t_{\nu} \langle \Phi_{\mu} | [H, \hat{\kappa}_{\nu}] | \Phi_{\mu} \rangle + o(\|\boldsymbol{t}\|),$$
(68)

which within our diagonal approximation of \hat{H} can be further approximated as:

$$E_{\mu}(\mathbf{t}) = E_{\mu}(0) + o(\|\mathbf{t}\|),$$
 (69)

and the same can be said of $E_0(t)$. We will from now on omit the term o(||t||).

Now, since we are interested in deriving an expression for $(J(\boldsymbol{t}^{(0)})^{-1}(J(\boldsymbol{t})-J(t^{(0)})))_{\mu,\nu}$ where $\boldsymbol{t}^{(0)}$ is the starting point of the quasi-Newton optimization, we need to have first an expression in first order of $\|\boldsymbol{t}^{(0)}\|$ of $J(\boldsymbol{t}^{(0)})^{-1}$.

Using (66) and (65), we can see that to first order:

$$J(\mathbf{t}^{(0)}) = D(I+S) \tag{70}$$

where $D = \operatorname{diag} \left(E_{\mu}(\boldsymbol{t}^{(0)}) - E_{0}(\boldsymbol{t}^{(0)}) \right)_{\mu,\nu}$ and $S = \left(\sum_{\nu'>\nu} t_{\nu'}^{(0)} \left\langle \Phi_{\mu} | \left[\hat{\kappa}_{\nu}, \hat{\kappa}_{\nu'} \right] | \Phi_{0} \right\rangle \right)_{\mu,\nu}$. Thus, we get that in first order, the inverse of $J(\boldsymbol{t}^{(0)})$ reads:

$$J(\mathbf{t}^{(0)})^{-1} = (I - S)D^{-1} \tag{71}$$

One can thus verify that in first order in both t and $\boldsymbol{t}^{(0)}$ we get:

$$J(\mathbf{t}^{(0)})^{-1}J(\mathbf{t})_{\mu,\nu} = \delta_{\mu,\nu} + \sum_{\nu'>\nu} (t_{\nu'} - t_{\nu'}^{(0)}) \langle \Phi_{\mu} | [\hat{\kappa}_{\nu}, \hat{\kappa}_{\nu'}] | \Phi_{0} \rangle$$
(72)

Thus:

$$\left(J(\mathbf{t}^{(0)})^{-1} \left(J(\mathbf{t}) - J(\mathbf{t}^{(0)})\right)\right)_{\mu,\nu} = \sum_{\nu' > \nu} (t_{\nu'} - t_{\nu'}^{(0)}) \left\langle \Phi_{\mu} | \left[\hat{\kappa}_{\nu}, \hat{\kappa}_{\nu'}\right] | \Phi_{0} \right\rangle \tag{73}$$

Since the parameter space is of finite dimension, we could choose any norm to determine L but it is best to use the norm for which the constant L in the end is the smallest. In what follows we use for simplicity the 1-norm $\|\cdot\|_1$ of \mathbb{R}^N , the associated operator norm of which is the 1-norm taken wrt. the columns, which we will also write $\|\cdot\|_1$. We get:

$$||J(\boldsymbol{t}^{(0)})^{-1}(J(\boldsymbol{t}) - J(\boldsymbol{t}^{(0)}))||_{1} = \sup_{\nu} \sum_{\mu \in \mathcal{A}} \left| \sum_{\nu' > \nu} (t_{\nu'} - t_{\nu'}^{(0)})' \left\langle \Phi_{\mu} | \left[\hat{\kappa}_{\nu}, \hat{\kappa}_{\nu'} \right] | \Phi_{0} \right. \right.$$

$$\leq \sup_{\nu} \sum_{\nu' > \nu} |t_{\nu'} - t_{\nu'}^{(0)}| \sum_{\mu \in \mathcal{A}} |\left\langle \Phi_{\mu} | \left[\hat{\kappa}_{\nu}, \hat{\kappa}_{\nu'} \right] | \Phi_{0} \right\rangle |$$

$$(75)$$

As discussed earlier, most of the commutators in the sum will be zero. To get a rough upper bound, one can notice that for each (ν, ν') there is at most one μ such that $\hat{\kappa}_{\nu}$ and $\hat{\kappa}_{\nu'}$ do not commute, and either $\hat{\kappa}_{\nu}\hat{\kappa}_{\nu'}|\Phi_{0}\rangle = \pm |\Phi_{\mu}\rangle \text{ or } \hat{\kappa}_{\nu'}\hat{\kappa}_{\nu}|\Phi_{0}\rangle = |\Phi_{\mu}\rangle. \text{ Therefore}$ we simply get:

$$||J(\mathbf{t}^{(0)})^{-1}(J(\mathbf{t}) - J(\mathbf{t}^{(0)}))||_1 \le ||\mathbf{t}||_1,$$
 (76)

and thus L=1.

This is the tightest upper bound on Eq. (74) if we consider t to be any point in a ball around $t^{(0)}$, but in general since many components of t are nonzero it is a somewhat rough upper bound, because for each ν not every $\nu' > \nu$ will result in a nonzero term $\sum_{\mu} |\langle \Phi_{\mu} | \left[\hat{\kappa}_{\nu}, \hat{\kappa}_{\nu'} \right] | \Phi_{0} \rangle |.$

About gradients

We are interested in establishing the relation:

$$\frac{\partial E_0}{\partial t_{\mu}}(\mathbf{t}) = 2r_{\mu}(\mathbf{t}) + O(\|\mathbf{t}\|) \tag{77}$$

One can easily check that using the notations we have previously introduced, we have:

$$\frac{\partial E_0}{\partial t_{\mu}}(\boldsymbol{t}) = \langle \Phi_0 | \left[\hat{U}(\boldsymbol{t})^{\dagger} \hat{H} \hat{U}(\boldsymbol{t}), \hat{\mathcal{U}}_{\nu}(\boldsymbol{t})^{\dagger} \hat{\kappa}_{\mu} \hat{\mathcal{U}}_{\nu}(\boldsymbol{t}) \right] | \Phi_0 \rangle,$$
(78)

which when using the value at t = 0 leaves us with:

$$\frac{\partial E_0}{\partial t_{\mu}}(\boldsymbol{t}) = \langle \Phi_0 | \left[\hat{H}, \hat{\kappa}_{\mu} \right] | \Phi_0 \rangle + O(\|\boldsymbol{t}\|) \tag{79}$$

$$=2r_{\mu}(\boldsymbol{t})+O(\|\boldsymbol{t}\|)\tag{80}$$

References

[1] Rajeev Acharya, Laleh Aghababaie-Beni, Igor Aleiner, Trond I. Andersen, Markus Ansmann, Frank Arute, Kunal Arya, Abraham Asfaw, Nikita Astrakhantsev, Juan Atalaya, Ryan Babbush, Dave Bacon, Brian Ballard, Joseph C. Bardin, Johannes Bausch, Andreas Bengtsson, Alexander Bilmes, Sam Blackwell, Sergio Boixo, Gina Bortoli, Alexandre Bourassa, Jenna Bovaird, Leon Brill, Michael Broughton, David A. Browne, Brett Buchea, Bob B. Buckley, David A. Buell, Tim Burger, Brian Burkett, Nicholas Bushnell, Anthony Cabrera, Juan Campero, Hung-Shen Chang, Yu Chen, Zijun Chen, Ben Chiaro, Desmond Chik, Charina Chou, Ja- $\sup_{\nu} \sum_{\mu \in A} \left| \sum_{\nu' > \nu} (t_{\nu'} - t_{\nu'}^{(0)})' \langle \Phi_{\mu} | [\hat{\kappa}_{\nu}, \hat{\kappa}_{\nu'}] | \Phi_{0} \rangle \right| \text{han Claes, Agnetta Y. Cleland, Josh Cogan, Roberto Collins, Paul Conner, William Court$ ney, Alexander L. Crook, Ben Curtin, Sayan Das, Alex Davies, Laura De Lorenzo, Dripto M. Debroy, Sean Demura, Michel Devoret, Agustin Di Paolo, Paul Donohoe, Ilya Drozdov, Andrew Dunsworth, Clint Earle, Thomas Edlich, Alec Eickbusch, Aviv Moshe Elbag, Mahmoud Elzouka, Catherine Erickson, Lara Faoro, Edward Farhi, Vinicius S. Ferreira, Leslie Flores Burgos, Ebrahim Forati, Austin G. Fowler, Brooks Foxen, Suhas Ganjam, Gonzalo Garcia, Robert Gasca, Élie Genois, William Giang, Craig Gidney, Dar Gilboa, Raja Gosula, Alejandro Grajales Dau, Dietrich Graumann, Alex Greene, Jonathan A. Gross, Steve Habegger, John Hall, Michael C. Hamilton, Monica Hansen, Matthew P. Harrigan, Sean D. Harrington, Francisco J. H. Heras, Stephen Heslin, Paula Heu, Oscar Higgott, Gordon Hill, Jeremy Hilton, George Holland, Sabrina Hong, Hsin-Yuan Huang, Ashley Huff, William J. Huggins, Lev B. Ioffe, Sergei V. Isakov, Justin Iveland, Evan Jeffrey, Zhang Jiang, Cody Jones, Stephen Jordan, Chaitali Joshi, Pavol Juhas, Dvir Kafri, Hui Kang, Amir H. Karamlou, Kostyantyn Kechedzhi, Julian Kelly, Trupti Khaire, Tanuj Khattar, Mostafa Khezri, Seon Kim, Paul V. Klimov, Andrey R. Klots, Bryce Kobrin, Pushmeet Kohli, Alexander N. Korotkov, Fedor Kostritsa, Robin Kothari, Borislav Kozlovskii, John Mark Kreikebaum, Vladislav D. Kurilovich, Nathan Lacroix, David Landhuis, Tiano Lange-Dei, Brandon W. Langley, Pavel Laptev, Kim-Ming Lau, Loïck Le Guevel, Justin Ledford, Kenny Lee, Yuri D. Lensky, Shannon Leon, Brian J. Lester, Wing Yan Li, Yin Li,

Alexander T. Lill, Wayne Liu, William P. Livingston, Aditya Locharla, Erik Lucero, Daniel Lundahl, Aaron Lunt, Sid Madhuk, Fionn D. Malone, Ashley Maloney, Salvatore Mandrá, Leigh S. Martin, Steven Martin, Orion Martin, Cameron Maxfield, Jarrod R. McClean, Matt McEwen, Seneca Meeks, Anthony Megrant, Xiao Mi, Kevin C. Miao, Amanda Mieszala, Reza Molavi, Sebastian Molina, Shirin Montazeri, Alexis Morvan, Ramis Movassagh, Wojciech Mruczkiewicz, Ofer Naaman, Matthew Neeley, Charles Neill, Ani Nersisyan, Hartmut Neven, Michael Newman, Jiun How Ng, Anthony Nguyen, Murray Nguyen, Chia-Hung Ni, Thomas E. O'Brien, William D. Oliver, Alex Opremcak, Kristoffer Ottosson, Andre Petukhov, Alex Pizzuto, John Platt, Rebecca Potter, Orion Pritchard, Leonid P. Pryadko, Chris Quintana, Ganesh Ramachandran, Matthew J. Reagor, David M. Rhodes, Gabrielle Roberts, Eliott Rosenberg, Emma Rosenfeld, Pedram Roushan, Nicholas C. Rubin, Negar Saei, Daniel Sank, Kannan Sankaragomathi, Kevin J. Satzinger, Henry F. Schurkus, Christopher Schuster, Andrew W. Senior, Michael J. Shearn, Aaron Shorter, Noah Shutty, Vladimir Shvarts, Shraddha Singh, Volodymyr Sivak, Jindra Skruzny, Spencer Small, Vadim Smelyanskiy, W. Clarke Smith, Rolando D. Somma, Sofia Springer, George Sterling, Doug Strain, Jordan Suchard, Aaron Szasz, Alex Sztein, Douglas Thor, Alfredo Torres, M. Mert Torunbalci, Abeer Vaishnav, Justin Vargas, Sergey Vdovichev, Guifre Vidal, Benjamin Villalonga, Catherine Vollgraff Heidweiller, Steven Waltman, Shannon X. Wang, Brayden Ware, Kate Weber, Theodore White, Kristi Wong, Bryan W. K. Woo, Cheng Xing, Z. Jamie Yao, Ping Yeh, Bicheng Ying, Juhwan Yoo, Noureldin Yosri, Grayson Young, Adam Zalcman, Yaxing Zhang, Ningfeng Zhu, and Nicholas Zobrist. Quantum error correction below the surface code threshold. 2024. URL http://arxiv.org/abs/2408.13687.

- [2] Ioannis Argyros. Approximating solutions of equations using newton's method with a modified newton's method iterate as a starting point. Rev. Anal. Numér. Théor. Approx., 36(2):123-137, Aug. 2007. URL https://ictp.acad.ro/jnaat/journal/article/view/2007-vol36-no2-art2.
- [3] Thomas Ayral, Pauline Besserve, Denis Lacroix, and Edgar Andres Ruiz Guzman. Quantum computing with and for many-body physics. The European Physical Journal A, 59(10):227, oct 2023. ISSN 1434-601X. DOI: 10.1140/epja/s10050-023-01141-1. URL http://arxiv.org/abs/2303.04850https://link.springer.com/10.1140/epja/

s10050-023-01141-1.

- [4] Rodney J. Bartlett and Monika Musiał. Coupled-cluster theory in quantum chemistry. <u>Rev. Mod. Phys.</u>, 79:291-352, Feb 2007. <u>DOI:</u> 10.1103/RevModPhys.79.291. URL https://link.aps.org/doi/10.1103/RevModPhys.79.291.
- [5] Pauline Besserve and Thomas Ayral. Unraveling correlated material properties with noisy quantum computers: Natural orbitalized variational quantum eigensolving of extended impurity models within a slave-boson approach. Physical Review B, 105(11):115108, mar 2022. ISSN 2469-9950. DOI: 10.1103/PhysRevB.105.115108. URL http://arxiv.org/abs/2108.10780https://link.aps.org/doi/10.1103/PhysRevB.105.115108.
- [6] Pauline Besserve, Michel Ferrero, and Thomas Ayral. Compact fermionic quantum state preparation with a natural-orbitalizing variational quantum eigensolving scheme. pages 1–15, jun 2024. URL http://arxiv.org/abs/2406. 14170.
- [7] M E Beverland, P Murali, M Troyer, K M Svore, T Hoefler, V Kliuchnikov, G H Low, M Soeken, A Sundaram, and A Vaschillo. Assessing requirements to scale to practical quantum advantage. pages 1–41, 2022.
- [8] Dolev Bluvstein, Simon J. Evered, Alexandra A. Geim, Sophie H. Li, Hengyun Zhou, Tom Manovitz, Sepehr Ebadi, Madelyn Cain, Marcin Kalinowski, Dominik Hangleiter, J. Pablo Bonilla Ataides, Nishad Maskara, Iris Cong, Xun Gao, Pedro Sales Rodriguez, Thomas Karolyshyn, Giulia Semeghini, Michael J. Gullans, Markus Greiner, Vladan Vuletić, and Mikhail D. Lukin. Logical quantum processor based on reconfigurable atom arrays. Nature, 626(7997):58-65, feb 2024. DOI: 10.1038/s41586-023-06927-0028-0836. 3. URL https://www.nature.com/articles/ s41586-023-06927-3.
- [9] M. P. da Silva, C. Ryan-Anderson, J. M. Bello-Rivas, A. Chernoguzov, J. M. Dreiling, C. Foltz, J. P. Gaebler, T. M. Gatterman, D. Hayes, N. Hewitt, J. Johansen, D. Lucchetti, M. Mills, S. A. Moses, B. Neyenhuis, A. Paz, J. Pino, P. Siegfried, J. Strabley, S. J. Wernli, R. P. Stutz, and K. M. Svore. Demonstration of logical qubits and repeated error correction with better-than-physical error rates. pages 1–13, 2024. URL http://arxiv.org/abs/2404.02280.
- [10] Francesco A. Evangelista, Garnet Kin-Lic Chan, and Gustavo E. Scuseria. Exact parameterization of fermionic wave functions via unitary coupled cluster theory. <u>The Journal of Chemical Physics</u>, 151(24), December 2019. ISSN 1089-7690. <u>DOI</u>:

- 10.1063/1.5133059. URL http://dx.doi.org/10.1063/1.5133059.
- [11] Richard P. Feynman. Simulating physics with computers. <u>International Journal of Theoretical Physics</u>, 21(6-7):467-488, jun 1982. ISSN 0020-7748. DOI: 10.1007/BF02650179. URL http://link.springer.com/10.1007/BF02650179.
- [12] Harper R. Grimsley, Sophia E. Economou, Edwin Barnes, and Nicholas J. Mayhall. An adaptive variational algorithm for exact molecular simulations on a quantum computer. Nature Communications, 10(1):3007, jul 2019. ISSN 2041-1723. DOI: 10.1038/s41467-019-10988-2. URL https://www.nature.com/articles/s41467-019-10988-2.
- [13] Mohammad Haidar, Marko J. Rančić, Thomas Ayral, Yvon Maday, and Jean-Philip Piquemal. Open Source Variational Quantum Eigensolver Extension of the Quantum Learning Machine (QLM) for Quantum Chemistry. <u>WIREs</u> Computational Molecular Science, in press, 2022. URL http://arxiv.org/abs/2206.08798.
- [14] Evans M Harrell. Generalizations of temple's inequality. Proceedings of the American Mathematical Society, 69(2):271–276, 1978. DOI: https://doi.org/10.1090/S0002-9939-1978-0487733-4.
- [15] Hsin-yuan Huang, Richard Kueng, and John Preskill. Predicting many properties of a quantum system from very few measurements. Nature Physics, 16(10):1050-1057, oct 2020. ISSN 1745-2473. DOI: 10.1038/s41567-020-0932-7. URL http://arxiv.org/abs/2002.08953http://dx.doi.org/10.1038/s41567-020-0932-7https://www.nature.com/articles/s41567-020-0932-7.
- [16] P. Jordan and E. Wigner. Über das paulische Äquivalenzverbot. Zeitschrift für Physik, 47(9): 631–651, 1928. DOI: 10.1007/BF01331938. URL https://doi.org/10.1007/BF01331938.
- [17] Abhinav Kandala, Antonio Mezzacapo, Kristan Temme, Maika Takita, Markus Brink, Jerry M. Chow, and Jay M. Gambetta. Hardware-efficient Variational Quantum Eigen-Small Molecules and Quantum solver for Nature, 549(7671):242-246, apr Magnets. 2017. ISSN 0028-0836. DOI: 10.1038/nature23879. URL http://www.nature.com/ doifinder/10.1038/nature23879http: //arxiv.org/abs/1704.05018http: //dx.doi.org/10.1038/nature23879.
- [18] A. Yu. Kitaev. Quantum measurements and the abelian stabilizer problem, 1995.
- [19] Jakob S. Kottmann, Abhinav Anand, and Alán Aspuru-Guzik. A feasible approach for automatically differentiable unitary coupled-cluster on quantum computers. <u>Chem. Sci.</u>, 12:3497–

- 3508, 2021. DOI: 10.1039/D0SC06627C. URL http://dx.doi.org/10.1039/D0SC06627C.
- [20] Sebastian Krinner, Nathan Lacroix, Ants Remm, Agustin Di Paolo, Elie Genois, Catherine Leroux, Christoph Hellings, Stefania Lazar, Francois Swiadek, Johannes Herrmann, Graham J Norris, Christian Kraglund Andersen, Markus Müller, Alexandre Blais, Christopher Eichler, and Andreas Wallraff. Realizing repeated quantum error correction in a distance-three surface code. Nature, 605(7911):669-674, may 2022. ISSN 0028-0836. DOI: 10.1038/s41586-022 - 04566 - 8. URL http://arxiv.org/abs/ 2112.03708http://dx.doi.org/10.1038/ s41586-022-04566-8https://www.nature. com/articles/s41586-022-04566-8.
- [21] Martin Larocca, Supanut Thanasilp, Samson Wang, Kunal Sharma, Jacob Biamonte, Patrick J Coles, Lukasz Cincio, Jarrod R. McClean, Zoë Holmes, and M Cerezo. A Review of Barren Plateaus in Variational Quantum Computing. pages 1–21, may 2024. URL http://arxiv.org/ abs/2405.00781.
- [22] Seunghoon Lee, Joonho Lee, Huanchen Zhai, Yu Tong, Alexander M. Dalzell, Ashutosh Kumar, Phillip Helms, Johnnie Gray, Zhi-Hao Cui, Wenyuan Liu, Michael Kastoryano, Ryan Babbush, John Preskill, David R. Reichman, Earl T. Campbell, Edward F. Valeev, Lin Lin, and Garnet Kin-Lic Chan. Evaluating the evidence for exponential quantum advantage in ground-state quantum chemistry. Nature Communications, 14(1):1952, 2023. ISSN 2041-1723. DOI: 10.1038/s41467-023-37587-6. URL http://arxiv.org/abs/ 2208.02199http://dx.doi.org/10.1038/ s41467-023-37587-6https://www.nature. com/articles/s41467-023-37587-6.
- [23] Seth Lloyd. Universal Quantum Simulators.
 Science, 273(5278):1073-1078, aug 1996. ISSN 0036-8075. DOI: 10.1126/science.273.5278.1073.
 URL https://www.science.org/doi/10.1126/science.273.5278.1073.
- [24] Thibaud Louvet, Thomas Ayral, and Xavier Waintal. On the feasibility of performing quantum chemistry calculations on quantum computers. 2023.
- [25] Jarrod R. McClean, Sergio Boixo, Vadim N. Smelyanskiy, Ryan Babbush, and Hartmut Neven. Barren plateaus in quantraining landscapes. tum neural network Novem-Nature Communications, 9(1),ber 2018. ISSN 2041-1723. DOI: 10.1038/s41467-018-07090-4.URL http: //dx.doi.org/10.1038/s41467-018-07090-4.
- [26] Jonathon P Misiewicz and Francesco A Evangelista. Implementation of the Projective Quantum

- Eigensolver on a Quantum Computer. 2023. URL https://arxiv.org/pdf/2310.04520.
- [27] Jonathon P. Misiewicz and Francesco A. Evangelista. Implementation of the projective quantum eigensolver on a quantum computer, 2023. URL https://arxiv.org/abs/2310.04520.
- [28] Wataru Mizukami, Kosuke Mitarai, Yuya O. Nakagawa, Takahiro Yamamoto, Tennin Yan, and Yu-ya Ohnishi. Orbital optimized unitary coupled cluster theory for quantum computer.

 Physical Review Research, 2(3):033421, sep 2020.

 ISSN 2643-1564. DOI: 10.1103/PhysRevResearch.2.033421. URL https://link.aps.org/doi/10.1103/PhysRevResearch.2.033421.
- [29] Javier Robledo Moreno, Jeffrey Cohn, Dries Sels, and Mario Motta. Enhancing the Expressivity of Variational Neural, and Hardware-Efficient Quantum States Through Orbital Rotations. pages 1–16, feb 2023. URL http: //arxiv.org/abs/2302.11588.
- [30] Jorge Nocedal and Stephen J. Wright. <u>Numerical Optimization</u>. Springer, New York, NY, USA, 2e edition, 2006. DOI: https://doi.org/10.1007/978-0-387-40065-5.
- [31] Alberto Peruzzo, Jarrod McClean, Peter Shadbolt, Man-Hong Yung, Xiao-Qi Zhou, Peter J. Love, Alán Aspuru-Guzik, and Jeremy L. O'Brien. A variational eigenvalue solver on a photonic quantum processor. Nature Communications, 5(1), July 2014. ISSN 2041-1723. DOI: 10.1038/ncomms5213. URL http://dx.doi.org/10.1038/ncomms5213.
- [32] Michael Ragone, Bojko N. Bakalov, Frédéric Sauvage, Alexander F. Kemper, Carlos Ortiz Marrero, Martin Larocca, and M. Cerezo. A Unified Theory of Barren Plateaus for Deep Parametrized Quantum Circuits. pages 33–37, sep 2023. URL http://arxiv.org/abs/2309. 09342.
- [33] Leonardo Ratini, Chiara Capecci, and Leonardo Guidoni. Optimization strategies in WAH-TOR algorithm for quantum computing empirical ansatz: a comparative study. pages 1–19, 2023. URL http://arxiv.org/abs/2306.11002.
- [34] Javier Robledo-Moreno, Mario Motta, Holger Haas, Ali Javadi-Abhari, Petar Jurcevic, William Kirby, Simon Martiel, Kunal Sharma, Sandeep Sharma, Tomonori Shirakawa, Iskandar Sitdikov, Rong-Yang Sun, Kevin J Sung, Maika Takita, Minh C Tran, Seiji Yunoki, and Antonio Mezzacapo. Chemistry Beyond Exact Solutions on a Quantum-Centric Supercomputer. may 2024. URL http://arxiv.org/abs/2405.05068.
- [35] Maria Schuld, Ville Bergholm, Christian Gogolin, Josh Izaac, and Nathan Killoran. Evaluating analytic gradients on quantum hardware. Physical Review A, 99

- (3), March 2019. ISSN 2469-9934. DOI: 10.1103/physreva.99.032331. URL http://dx.doi.org/10.1103/PhysRevA.99.032331.
- [36] Nicholas H. Stair and Francesco A. Evangelista. Simulating many-body systems with a projective quantum eigensolver. PRX Quantum, 2(3), jul 2021. DOI: 10.1103/prxquantum.2.030301. URL https://doi.org/10.1103%2Fprxquantum.2.030301.
- [37] Jules Tilly, Hongxiang Chen, Shuxiang Cao, Dario Picozzi, Kanav Setia, Ying Li, Edward Grant, Leonard Wossnig, Ivan Rungger, George H. Booth, and Jonathan Tennyson. The variational quantum eigensolver: A review of methods and best practices. Physics Reports, 986:1–128, November 2022. ISSN 0370-1573. DOI: 10.1016/j.physrep.2022.08.003. URL http://dx.doi.org/10.1016/j.physrep. 2022.08.003.
- [38] Dave Wecker, Bela Bauer, Bryan K. Clark, Matthew B. Hastings, and Matthias Troyer. Gate-count estimates for performing quantum chemistry on small quantum computers. Physical Review A, 90(2):022305, aug 2014. ISSN 1050-2947. DOI: 10.1103/Phys-RevA.90.022305. URL https://link.aps.org/doi/10.1103/PhysRevA.90.022305.
- [39] Dave Wecker, Matthew B. Hastings, and Matthias Troyer. Progress towards practical quantum variational algorithms. Physical Review A, 92(4), October 2015. ISSN 1094-1622.

 DOI: 10.1103/physreva.92.042303. URL http://dx.doi.org/10.1103/PhysRevA.92.042303.
- [40] Dan-Bo Zhang, Zhan-Hao Yuan, and Tao Yin. Variational quantum eigensolvers by variance minimization, 2020. URL https://arxiv.org/ abs/2006.15781.
- [41] Jiří Čížek. On the Correlation Problem in Atomic and Molecular Systems. Calculation of Wavefunction Components in Ursell-Type Expansion Using Quantum-Field Theoretical Methods. The Journal of Chemical Physics, 45(11): 4256–4266, 12 1966. ISSN 0021-9606. DOI: 10.1063/1.1727484. URL https://doi.org/10.1063/1.1727484.